Molecular Pharmacology Fast Forward. Published on February 7, 2018 as DOI: 10.1124/mol.117.109975
This article has not been copyedited and formatted. The final version may differ from this version.

Allosterism within delta opioid-kappa opioid receptor heteromers in peripheral sensory neurons: Regulation of kappa opioid agonist efficacy

Blaine A. Jacobs, Miryam M. Pando, Elaine Jennings, Teresa A. Chavera, William P. Clarke and Kelly A. Berg*

Department of Pharmacology

The University of Texas Health Science Center at San Antonio

7703 Floyd Curl Drive, San Antonio, TX 78229-3900 USA

Molecular Pharmacology Fast Forward. Published on February 7, 2018 as DOI: 10.1124/mol.117.109975
This article has not been copyedited and formatted. The final version may differ from this version.

Running Title Page

a) **Running Title:** Regulation of agonist efficacy at DOR-KOR heteromers

b) **Corresponding author:**

Kelly A. Berg

Department of Pharmacology-MS7764

The University of Texas Health Science Center at San Antonio

7703 Floyd Curl Drive

San Antonio, TX 78229-3900

Voice: (210)-567-3528

Email: berg@uthscsa.edu

c) **Number of Text pages**: 20

Number of tables: 0

Number of figures: 9

Supplemental figures: 9

Number of references: 40

Word count

Abstract: 250

Introduction: 698

Discussion: 1518

Molecular Pharmacology Fast Forward. Published on February 7, 2018 as DOI: 10.1124/mol.117.109975
This article has not been copyedited and formatted. The final version may differ from this version.

d) Non-standard abbreviations:

6-GNTI, 6'-guanidinonaltrindole; **AC**, adenylyl cyclase; **BK**, bradykinin; **BNTX**, 7-benzylidenaltrexone; **DAMGO**, [D-Ala^2,*N*-MePhe^4,Gly-ol^5]-enkephalin; **DOR**, delta opioid receptor; **DPDPE**, [D-Pen^{2,5}]-Enkephalin; **GPCR**, G protein coupled receptor; **i.pl**., intraplantar; **KOR**, kappa opioid receptor; **NTB**, naltriben; **NTI**, naltrindole; **PGE_2** , prostaglandin E2; **PWL**, paw withdrawal latency; **TAT**, transactivator of transcription peptide; **TM1**, transmembrane domain 1.

Molecular Pharmacology Fast Forward. Published on February 7, 2018 as DOI: 10.1124/mol.117.109975
This article has not been copyedited and formatted. The final version may differ from this version.

Abstract

There is abundant evidence for formation of G protein coupled receptor heteromers in heterologous expression systems, however, little is known of the function of heteromers in native systems. Heteromers of delta and kappa opioid receptors (DOR-KOR heteromers) have been identified in native systems. We previously reported that activation of DOR-KOR heteromers expressed by rat pain-sensing neurons (nociceptors) produces robust, peripherally-mediated antinociception. Moreover, DOR agonist potency and efficacy is regulated by KOR antagonists via allosteric interactions within the DOR-KOR heteromer in a ligand-dependent manner. Here we assessed the reciprocal regulation of KOR agonist function by DOR antagonists in adult rat nociceptors in culture and in a behavioral assay of nociception. Naltrindole enhanced the potency of the KOR agonist ICI-199441 (10-20 fold), but did not alter responses to U50488. By contrast, the potency of U50488 was enhanced (20 fold) by 7-benzylidenenaltrexone. The efficacy of 6'-guanidinonaltrindole (6'-GNTI) to inhibit nociceptors was blocked by siRNA knock-down of DOR or KOR. Replacing 6'-GNTI occupancy of DOR with either naltrindole or 7-benzylidenenaltrexone abolished 6'-GNTI efficacy. Further, peptides derived from DOR transmembrane segment 1, fused to the cell membrane penetrating HIV transactivator of transcription peptide, also blocked 6'-GNTI-mediated responses ex vivo and in vivo, suggesting that 6'-GNTI efficacy in nociceptors is due to its positive allosteric regulation of KOR via occupancy of DOR in a DOR-KOR heteromer. Together, these results provide evidence for the existence of functional DOR-KOR heteromers in rat peripheral sensory neurons and that reciprocal, ligand-dependent, allosteric interactions occur between the DOR and KOR protomers.

Molecular Pharmacology Fast Forward. Published on February 7, 2018 as DOI: 10.1124/mol.117.109975
This article has not been copyedited and formatted. The final version may differ from this version.

Introduction

There is considerable evidence that G protein coupled receptors (GPCRs) form heteromers (Gomes et al., 2016). However, compared with the large amount of data for heteromers obtained with heterologous expression systems, there is relatively little evidence for a role for heteromers in regulating function in physiologically-relevant systems. In part, this may be due to limitations in the applicability of the techniques/approaches to study heteromers in native tissues. GPCR heteromers are of interest as drug targets because they can have unique pharmacological properties and their restricted cellular/tissue distribution (heteromers can form only in cells that co-express both protomers) provides for selectivity. Because heterologous systems do not always adequately model the cellular context of receptors expressed in native systems and cannot model the physiological environment and complexity of integrated response systems that exist in vivo, it is important that more work be done to understand the role of heteromers in physiologically-relevant systems.

Among the unique pharmacological characteristics associated with heteromers are the allosteric interactions that can occur between the protomers. It has been shown that the presence of one protomer can alter membrane localization (Ellis et al., 2006; Rozenfeld et al., 2012), the affinity and/or efficacy of agonists (Martin and Prather, 2001; Rozenfeld et al., 2012; Wang et al., 2005), and signaling specificity (Charles et al., 2003; Rozenfeld et al., 2012) for the other promoter. Moreover, ligand binding to the orthosteric site of one promoter can change the pharmacological properties of orthosteric ligands for the other protomer (Ferre et al., 2016; Shivnaraine et al., 2016; Vischer et al., 2011). For example, apelin binding to its receptor reduces the binding and efficacy of angiotensin II acting at the angiotensin II Type 1 receptor via negative cooperativity between the protomers of the heteromer (Siddiquee et al., 2013). Guitart et al (2014) showed synergy for dopamine D1 and D3 receptor agonists to stimulate extracellular signal-regulated kinase activation, but not for adenylyl cyclase activity, and this

Molecular Pharmacology Fast Forward. Published on February 7, 2018 as DOI: 10.1124/mol.117.109975
This article has not been copyedited and formatted. The final version may differ from this version.

synergistic response was blocked by transmembrane peptides that blocked heteromer formation. Thus, orthosteric ligands for one protomer can act as allosteric regulators that influence affinity, efficacy and signaling specificity of orthosteric ligands for the other protomer of a heteromer.

Several studies have shown that delta and kappa opioid receptors (DOR and KOR, respectively) can form heteromers in heterologous expression systems (Jordan and Devi, 1999; Waldhoer et al., 2005; Xie et al., 2005) and there is also evidence for functional DOR-KOR heteromers in spinal cord (Ansonoff et al., 2010; Waldhoer et al., 2005). Recently, we provided evidence for functional DOR-KOR heteromers in peripheral pain-sensing neurons (nociceptors) in primary cultures and in vivo (Berg et al., 2012). We found that KOR co-immunoprecipitated with DOR from cultures of adult rat sensory neurons from the trigeminal ganglia and that a DOR-KOR heteromer-selective antibody augmented the antinociceptive efficacy of the DOR agonist, [D-Pen^{2,5}]-enkephalin (DPDPE). Moreover, we found that antagonists selective for KOR altered the potency and/or efficacy of selective DOR agonists in a ligand-dependent manner both in sensory neuron cultures and in behavioral antinociception tests in vivo. Such ligand-dependent effects are a hallmark of allosterism (Christopoulos et al., 2014; Smith and Milligan, 2010). These results suggested a functional role for DOR-KOR heteromers in rat sensory neurons and that orthosteric KOR ligands regulated the function of orthosteric DOR ligands via intra-heteromer allosteric interactions.

In addition to ligand-dependence, another hallmark of allosterism is reciprocity (Smith and Milligan, 2010). Thus, it is expected that if KOR antagonist regulation of DOR agonist function is due to intra-heteromer allosteric regulation, then DOR ligands should regulate the function of KOR agonists. In this study, we examined the effects of DOR antagonists on KOR agonist-mediated inhibition of rat peripheral sensory neurons in culture and in vivo. We found that DOR antagonists altered the function of KOR agonists in a ligand-dependent manner.

Molecular Pharmacology Fast Forward. Published on February 7, 2018 as DOI: 10.1124/mol.117.109975
This article has not been copyedited and formatted. The final version may differ from this version.

Moreover, we discovered that the putative DOR-KOR heteromer-selective activity of 6'-GNTI in peripheral sensory neurons was due to allosteric enhancement of 6'-GNTI efficacy at KOR via its occupancy of DOR and that this effect was blocked by DOR transmembrane peptides both in culture and in vivo. Taken together, these results provide strong evidence for a functional role of DOR-KOR heteromers in regulating the activity of rat peripheral pain-sensing neurons.

Molecular Pharmacology Fast Forward. Published on February 7, 2018 as DOI: 10.1124/mol.117.109975
This article has not been copyedited and formatted. The final version may differ from this version.

Materials and Methods

Materials. 6'-GNTI, U50488, and naltrindole (NTI), and rolipram were purchased from Sigma-Aldrich (St. Louis, MO). DPDPE, D-Ala^2,*N*-MePhe^4,Gly-ol^5]-enkephalin (DAMGO), and bradykinin (BK) were purchased from Bachem Americas, Inc. (Torrance, CA). ICI-199441, 7-benzylidenaltrexone (BNTX) and naltriben (NTB) were purchased from Tocris (Minneapolis, MN). PGE_2 was purchased from Cayman Chemicals (Ann Arbor, MI). ^{125}I-cAMP was purchased from PerkinElmer Life and Analytical Sciences (Waltham, MA). Nerve growth factor (NGF) was from Harlan (Houston, TX). Collagenase was from Worthington (Lakewood, NJ). ON-TARGET plus SMART pool rat siRNAs and Dharmafect transfection reagent were from GE Dharmacon (Pittsburgh, PA). Hank's balanced salt solution, fetal bovine serum (FBS), and Dulbecco's modified Eagles Medium (DMEM) were purchased from Invitrogen Corp. (Carlsbad, CA). Dr. Philip S. Portoghese provided the bivalent KOR agonist/DOR antagonist ligand KDAN-18. All other drugs and chemical (reagent grade) were purchased from Sigma-Aldrich.

Animals. Adult male Sprague-Dawley rats (Charles River Laboratories, Wilmington MA) weighing 250 to 300 g were used in this study. The animal study protocol was approved by the Institutional Animal Care and Use Committee of the University of Texas Health Science Center at San Antonio and conformed to International Association for the Study of Pain and federal guidelines. Animals were housed for 1 week with food and water available ad libitum before behavioral testing or harvesting of sensory neurons of the trigeminal ganglia.

Behavioral assay of nociception. Opioid agonist-mediated inhibition of prostaglandin E_2 (PGE_2)-induced thermal allodynia was measured as described previously (Berg et al., 2012; Berg et al., 2011; Rowan et al., 2009; Sullivan et al., 2015). Paw withdrawal latency (PWL) in response to application of a thermal stimulus to the ventral surface of the rat hindpaw was measured with a plantar test apparatus (Hargreaves et al., 1988). In brief, rats were placed in

Molecular Pharmacology Fast Forward. Published on February 7, 2018 as DOI: 10.1124/mol.117.109975
This article has not been copyedited and formatted. The final version may differ from this version.

plastic boxes with a glass floor maintained at 30°C. After a 30 min habituation period, the plantar surface of the hindpaw was exposed to a narrow beam (approximately 5 mm diameter) of radiant heat through the glass floor. The intensity of the thermal stimulus was adjusted so that baseline PWL values were 10 ± 2 s with a cut-off time of 25 s. All drugs were dissolved in phosphate-buffered saline and administered via intraplantar (i.pl.) injection (50 µl) into the rat hindpaw. To induce thermal allodynia, PGE_2 (0.3 µg, i.pl.) was injected. We have shown previously that this dose of PGE_2 produces a mild (≈5 second reduction in PWL) and prolonged (>20 minutes) thermal allodynia (Rowan et al., 2009). Opioid agonists, or vehicle, were co-injected (i.pl.) with PGE_2. PWL measurements were taken in duplicate at least 30 s apart at 5 min intervals before injections (baseline) and for 20 min after the last injection by observers blinded to treatment allocation. As opioid receptors expressed by peripheral sensory neurons require an inflammatory stimulus for antinociceptive efficacy (Berg et al., 2007; Berg et al., 2012; Berg et al., 2011; Jamshidi et al., 2015; Rowan et al., 2009; Stein and Lang, 2009; Stein and Zollner, 2009; Sullivan et al., 2015), all experiments were done using pre-treatment (15 min) with bradykinin (BK, 25 µg, i.pl.) to induce opioid receptor functional competence. Injection of BK produces a transient allodynia that returns to baseline within 10 min (before administration of PGE_2 ± opioid) (see Supplemental Figures 4-6, 8-9). To verify that behavioral responses were due to local, peripherally restricted doses of a given agonist, PWL in the contralateral paw was measured after i.pl. injection into the ipsilateral paw (Berg et al., 2012; Berg et al., 2011; Rowan et al., 2009).

Primary cultures of peripheral sensory neurons. Primary cultures derived from adult rat trigeminal ganglia were prepared as described previously (Berg et al., 2007; Berg et al., 2012; Jamshidi et al., 2015). Cultures were refed with DMEM containing 10% FBS, 1% penicillin-streptomycin, 1% GlutaMAX I, 1% mitotic inhibitors (5-fluor-2-deoxyuridine, uridine) and 100 ng

Molecular Pharmacology Fast Forward. Published on February 7, 2018 as DOI: 10.1124/mol.117.109975
This article has not been copyedited and formatted. The final version may differ from this version.

nerve growth factor every 48h. Cultures were refed with DMEM without NGF or FBS (i.e. serum free media) 24 h before experiments performed between 6-8 days in culture.

siRNA transfection. Primary cultures of peripheral sensory neurons (3 days in culture) were transfected with ON-TARGET plus SMART pool rat siRNA (50 nM) directed against DOR (cat # L-080122-02), KOR (cat # L-090460-02) or non-targeting siRNA (cat # D-001810-10-05) using DharmaFECT 3 transfection reagent according to the manufacturers protocol. Cultures were refed with complete media 24 h and 72 h after transfection. Cells were refed with serum free media 4 days after siRNA transfection and experiments done 24 h later.

RT-qPCR analysis of mRNA levels. siRNA-mediated reduction in DOR or KOR mRNA levels was determined 48 h and 5 days after siRNA transfection. Total RNA was isolated using the PureLink RNA Mini Kit (Life Technologies) and treated with DNAse (Qiagen RNAse-free DNAse set). RNA concentrations were measured using the Nanodrop 2000 (Thermo Scientific) and samples were normalized for equal RNA quantity. Reverse transcription was done following the manufacturer's protocol using High Capacity cDNA Reverse Transcription Kit (Applied Biosystems). Pre-designed DOR (Forward 5'-CCA GCT GGT ACT GGG ACA CT-3'; Reverse 5'- CGA TGA CGA AGA TGT GGA TG-3'), KOR (Forward 5'- TTG GCC TTT TGG AGA TGT TC-3'; Reverse 5'- TGG TGC CTC CAA GGA CTA TC-3'), and the housekeeping gene and endogenous control actin (Forward 5'- AGC CAT GTA CGT AGC CAT CC-3' Reverse 5'- ACC CTC ATA GAT GGG CAC AG-3') primers were purchased from Invitrogen. Reactions were performed in triplicate containing 2× SsoFast™ EvaGreen®Supermix (Bio-Rad) and quantitative real-time PCR was performed using the PE 9600 thermal cycler (Perkin Elmer, Biosystems). A 'no template' control reaction was included in all assays. The relative expression of target genes to endogenous control was calculated using the formula $2^{-\Delta\Delta Ct}$, where ΔCt represents the magnitude of the difference between target and endogenous control cycle threshold (Ct) values. The values are expressed as fold change relative to the control.

Molecular Pharmacology Fast Forward. Published on February 7, 2018 as DOI: 10.1124/mol.117.109975
This article has not been copyedited and formatted. The final version may differ from this version.

Measurement of cellular cAMP levels. Opioid receptor-mediated inhibition of adenylyl cyclase activity was determined by measuring the amount of cAMP accumulated in cells treated with the Gs protein-coupled prostaglandin receptor agonist, PGE_2 and an opioid agonist in the presence of the phosphodiesterase inhibitor, rolipram, as previously described (Berg et al., 2007; Berg et al., 2012; Jamshidi et al., 2015). As described above for the behavioral experiments, cells were pre-treated for 15 min with BK to induce opioid receptor functional competence. Cells were washed twice with HBSS containing 20 mM HEPES, pH 7.4 (wash buffer) followed by pre-incubation in wash buffer (250 µl per well, 48 well plate) for 15 min at 37°C with BK (10 µM). To assess opioid agonist-mediated responses, cells were incubated with rolipram (0.1 mM) along with a maximal concentration of PGE_2 (1 µM) with opioid ligands or vehicle for 15 min at 37°C. Incubations were terminated by aspiration of the buffer and addition of 500 µl ice cold absolute ethanol. The ethanol extracts from individual wells were dried under a gentle air stream and reconstituted in 100 µl 50 mM sodium acetate, pH 6.2. The cAMP content of each well was determined by radioimmunoassay.

DOR transmembrane peptides. Peptides consisting of residues corresponding to the first transmembrane (TM) spanning domain of DOR (AITALYSAVCAVGLLGNVLVMFGI), fused to the cell membrane penetrating HIV transactivator of transcription (TAT), peptide (YGRKKRRQRRRPQ) (Brooks et al., 2005) were synthesized (95% purity) by Lieftein LLC (Hillsborough, NJ). For insertion of the DOR TM1-TAT peptide in the proper orientation (i.e., same direction as that of TM1 in native DOR), the TAT sequence was fused to the C-terminus of the peptide. As a negative control, the TAT sequence was fused to the N-terminus of the DOR TM1 peptide (TAT-TM1) so membrane insertion would occur in the opposite direction of the native DOR TM1 (He et al., 2011). For behavioral experiments, TM-TAT peptides were dissolved in sterile PBS (78.8 µg/ml) and rats received 50 µl (3.94 µg) i.pl. 30 min before testing for opioid agonist-mediated inhibition of PGE_2-stimulated thermal allodynia. BK was co-injected

Molecular Pharmacology Fast Forward. Published on February 7, 2018 as DOI: 10.1124/mol.117.109975
This article has not been copyedited and formatted. The final version may differ from this version.

with the TM-TAT peptides. Based upon a paw volume of distribution of 1 ml, the approximate concentration of the peptides was 1 μM. For cell culture experiments, the peptides were dissolved in sterile HBSS (10 μM) and used at a final concentration of 1 μM.

Data Analysis. All statistical analyses were done using Prism software (GraphPad Software, Inc., San Diego, CA, version 6.0). For cell culture experiments, concentration-response data were fit to a logistic equation (Eq. 1) using non-linear regression analysis to provide estimates of maximal response (E_{max}), and potency (EC_{50}).

Eq. 1: $$R= R_o – ((R_o – R_i)/(1 + ([A]/EC_{50}))$$

Where R is the measured response at a given agonist concentration (A), R_o is the response in the absence of agonist, R_i is the response after maximal inhibition by the agonist, and EC_{50} is the concentration of agonist that produces a half-maximal response. The maximal effect of an agonist was calculated as Ro-Ri. Experiments were repeated at least four times, in triplicate, using cells obtained from different groups of rats. Statistical analysis of treatments on EC_{50} and E_{max} parameters, determined from individual curve fits, were done with a paired *t* test. When only a single drug concentration was used, statistical analysis was done with one-way ANOVA followed by Dunnett's post test. $P < 0.05$ was considered statistically significant.

For behavior experiments, monotonic dose response curve data were evaluated using non-linear regression analysis (Equation 1). The significance of treatment effects on the mean fit values for ED_{50} and E_{max} parameters were determined with an F test. To determine statistical differences of U50488 "U"-shaped dose response curves in the presence or absence of antagonists, data were analyzed by two-way ANOVA (two factors were dose and treatment) followed by Bonferroni's post test. All time course data were analyzed for statistical significance using two-way ANOVA (two factors were dose and time) followed by Bonferroni's post test. Statistical analyses of PWL data 10 min following injection were done using one-way ANOVA

Molecular Pharmacology Fast Forward. Published on February 7, 2018 as DOI: 10.1124/mol.117.109975
This article has not been copyedited and formatted. The final version may differ from this version.

followed by Dunnett's post test. Unless otherwise stated, data are presented as mean ± SEM of at least 6 rats per group. *P* values < 0.05 were considered statistically significant.

Molecular Pharmacology Fast Forward. Published on February 7, 2018 as DOI: 10.1124/mol.117.109975
This article has not been copyedited and formatted. The final version may differ from this version.

Results

Allosteric regulation of KOR agonist-mediated responses by DOR antagonists in peripheral nociceptors ex vivo and in vivo.

Ligand-dependent effects of DOR antagonists on KOR agonist responses.

As shown in Figure 1A, the concentration-response curve (CRC) for the KOR agonist, ICI-199441, for inhibition of PGE_2-stimulated cAMP accumulation in cultures of sensory neurons, was shifted to the left approximately 20-fold with no change in the E_{max} by the DOR antagonist, naltrindole (NTI; 20 nM, 100 x Ki for DOR, (Clark et al., 1997)). The mean pEC_{50} was 7.94 ± 0.24 (11 nM) versus 9.27 ± 0.42 (0.5 nM), Veh and NTI, respectively, mean ± SEM of 5 individual curves, (paired t-test, $P < 0.05$). The mean maximal inhibition of PGE_2-stimulated cAMP levels for ICI-199441 was 40 ± 3% vs. 37 ± 2%, mean ± SEM for Veh and NTI, respectively, n=5 (paired t-test, $P = 0.96$). As we have found previously (Berg et al., 2011; Jamshidi et al., 2015), neither basal nor PGE_2-stimulated cAMP levels were altered by NTI alone (see legend of Figure 1). To confirm effective receptor occupancy of DOR we measured effects of NTI on inhibition of cAMP accumulation by maximal concentrations of the DOR agonist, DPDPE (100 nM). As shown in Supplemental Figure 1, the DPDPE-mediated response was blocked completely by 20 nM NTI.

To further probe the allosteric effect of the DOR antagonist, NTI, on the response to the KOR agonist, ICI-199441, we examined the concentration dependence of NTI to enhance a subthreshold concentration of ICI-199441. As shown in Supplemental Figure 2, incubation with 1 nM ICI-199441 had no effect on PGE_2-stimulated cAMP accumulation alone. By contrast, in cells pretreated with NTI (0.2-100 nM), PGE_2-stimulated cAMP levels were reduced by 1 nM ICI-100441 in an NTI concentration-dependent manner, with an EC_{50} value of 0.4 nM, which is consistent with the affinity reported for NTI (Clark et al., 1997). Maximal enhancement of the

Molecular Pharmacology Fast Forward. Published on February 7, 2018 as DOI: 10.1124/mol.117.109975
This article has not been copyedited and formatted. The final version may differ from this version.

response to 1 nM ICI-199441 occurred with 20 nM NTI, with no further enhancement with higher concentrations of NTI (100 nM) indicating that the concentration-dependent effect of the DOR antagonist was limited, a hallmark of an allosteric effect (Christopoulos et al., 2014; Kenakin, 2009; Smith and Milligan, 2010). Importantly, in this experiment, the inhibition of PGE_2-stimulated cAMP accumulation by 1 nM ICI-199441 in the presence of maximally enhancing concentrations of NTI was less than that produced with a maximal concentration of ICI alone (1 μM), indicating that the plateau in the NTI-mediated enhancement was not due to a floor effect (see Supplemental Figure 2). The magnitude of inhibition produced by 1 nM ICI-199441 in the presence of 20 nM NTI, relative to 1 μM ICI-199441, differed between experiments (Figure 1A and Supplemental Figure 2). Such variability may be attributable to differences in primary neuronal cultures (e.g., differences in receptor reserve) prepared at different times over the course of this study.

By contrast, NTI did not alter inhibition of PGE_2-stimulated cAMP accumulation produced by the KOR agonist, U50488 (Figure 1B). The mean pEC_{50} values for U50488 were 8.74 ± 0.32 (2 nM) vs. 8.46 ± 0.41 (3 nM) for Veh vs. NTI, respectively (paired t-test, P = 0.71; n=5). The mean maximal inhibition of PGE_2-stimulated cAMP accumulation was 55 ± 5% vs. 62 ± 1% for Veh vs. NTI, respectively, (paired t-test, P =0.29; n=5).

In the behavioral model of thermal nociception, the effect of NTI on KOR agonist-mediated anti-allodynia was also dependent on the KOR agonist. As shown in Figure 2A, local injection (i.pl.) of ICI-199441 dose-dependently inhibited PGE_2-evoked thermal allodynia (increased PWL). In the presence of NTI (40 μg, i.pl.), a dose that we have used before to block DOR agonist effects (Berg et al., 2012; Rowan et al., 2009) and see Supplemental Figure 3), the ICI-199441 dose response curve (DRC) was shifted to the left approximately 10-fold. The ED_{50} for ICI-1994411 was 1.8 μg vs. 0.14 μg for Veh vs. NTI, respectively ($F_{(1,81)}$ = 5.428, P = 0.02).

Molecular Pharmacology Fast Forward. Published on February 7, 2018 as DOI: 10.1124/mol.117.109975
This article has not been copyedited and formatted. The final version may differ from this version.

We next tested the effect of NTI on the response to the KOR agonist, U50488. We have previously reported that the DRC for U50488 for reduction of PGE_2-evoked thermal allodynia has an inverted "U" shape (Berg et al., 2011) and that the descending limb is due to U50488-mediated activation of the mitogen-activated protein kinase, extracellular signal-regulated kinase (Jamshidi et al., 2015). KOR agonists that do not activate mitogen-activated protein kinase have a monotonic DRC (Jamshidi et al., 2015). Consistent with our previous findings, the DRC for U50488 was an inverted "U" shape (Figure 2B). By contrast to the effect of ICI-199441, the DRC for U50488-mediated inhibition of PGE_2-evoked thermal allodynia was not altered by NTI (Figure 2B). In the presence of NTI, there was no change in either the ascending or descending limb of the U50488 DRC (Figure 2B) ($F_{(1,59)}$ = 0.81, P = 0.37). As shown in Supplemental Figure 3, injection of NTI produced complete blockade of a maximal dose of DPDPE for reduction of PGE_2-evoked thermal allodynia.

We next tested effects of a different DOR antagonist, BNTX, on the U50488–mediated response in the behavioral model of thermal nociception. Based on an estimated rat paw volume of distribution of 1 ml, injection of a 1 µg dose of BNTX would approximate 200 nM, a concentration of about 100 x Ki for DOR (Neilan et al., 1999; Raynor et al., 1994). As shown in Supplemental Figure 3, i.pl. injection of 1 µg BNTX blocked completely a maximal dose of DPDPE to inhibit PGE_2-evoked thermal allodynia, indicating occupancy of DOR with this dose of BNTX. Injection of BNTX with U50488 shifted the U50488 DRC significantly to the left (Figure 3) ($F_{(1, 121)}$ = 4.08, P= 0.04). Because there is only a 10-fold affinity difference of BNTX for DOR and MOR (Raynor et al., 1994), we tested whether the enhancing effect of BNTX was due to occupancy of DOR by determining if NTI was able to block the BNTX-mediated shift in the U50488 DRC. As shown in Figure 3, co-injection of NTI (40 µg, i.pl) along with BNTX blocked completely the shift in the U50488 DRC ($F_{(1,89)}$ = 3.177, P = 0.08). As presented above, NTI did

Molecular Pharmacology Fast Forward. Published on February 7, 2018 as DOI: 10.1124/mol.117.109975
This article has not been copyedited and formatted. The final version may differ from this version.

not alter the DRC for U50488-mediated reduction in thermal allodynia when tested alone (Figure 2).

The DOR-KOR heteromer selectivity of 6'-GNTI in peripheral sensory neurons is due to allosteric interactions between the DOR and KOR protomers.

Agonist efficacy of 6'-GNTI requires expression of both DOR and KOR

We have previously shown that 6'-GNTI acts as an agonist for inhibition of PGE_2-stimulated cAMP accumulation in primary cultures of peripheral sensory neurons as well as for reduction in PGE_2–induced thermal allodynia in vivo (Berg et al., 2012). These actions of 6'-GNTI are blocked by antagonists of either DOR or KOR (Berg et al., 2012). To confirm that agonism of 6'-GNTI requires occupancy of both DOR and KOR, we tested the effect of knock-down of DOR or KOR using siRNA on 6'-GNTI-mediated inhibition of PGE_2 -stimulated cAMP accumulation. Transfection of peripheral sensory neuron cultures with siRNA directed against DOR (or non-targeting siRNA) resulted in a decrease in DOR mRNA (normalized to actin) by 1.5- and 2.2-fold measured 2 and 5 days later, respectively, compared to control as measured by qPCR. Similarly, KOR mRNA was decreased 1.65- and 1.92-fold vs. control measured 2 and 5 days after siRNA transfection, respectively. As shown in Figure 4A, 5 days after treatment with KOR siRNA, the response to a maximal concentration of U50488 was abolished. By contrast, KOR siRNA treatment had no effect on the response to DPDPE (Figure 4B). Similarly, 5 days after treatment with DOR siRNA (Figure 4B) the response to DPDPE was abolished, however, DOR siRNA treatment had no effect on the response to U50488 (Figure 4A). Treatment with either DOR or KOR siRNA did not alter inhibition of adenylyl cyclase activity by a maximal concentration of the MOR agonist, DAMGO (1 μM) (Figure 4C). By contrast, 6'-GNTI-mediated inhibition of PGE_2-stimulated cAMP accumulation was abolished following treatment with either siRNA for DOR or siRNA for KOR (Figure 4D).

Molecular Pharmacology Fast Forward. Published on February 7, 2018 as DOI: 10.1124/mol.117.109975
This article has not been copyedited and formatted. The final version may differ from this version.

We also tested the effects of DOR and KOR siRNA treatment on inhibition of PGE_2-stimulated cAMP accumulation by the putative DOR-KOR heteromer bivalent ligand, KDAN-18, which is comprised of the KOR agonist, ICI-199411 linked to the DOR antagonist, NTI (Ansonoff et al., 2010; Daniels et al., 2005). As shown in Supplemental Figure 7, responsiveness to KDAN-18 was abolished following siRNA knockdown of either DOR or KOR.

6'-GNTI has antagonist properties at both DOR and KOR in the absence of co-expression

To determine if 6'-GNTI occupied DOR or KOR in the absence of the corresponding receptor, we measured the effect of 6'-GNTI on CRCs to DPDPE or U50488 following siRNA-mediated knockdown of either DOR or KOR expression. In cells transfected with DOR siRNA, 6'-GNTI antagonized U50488-mediated inhibition of PGE_2-stimulated cAMP accumulation (Figure 5A, $F_{(1,42)} = 44.23$, $P < 0.0001$) demonstrating occupancy of KOR by 6'-GNTI. Similarly, in cells transfected with KOR siRNA, 6'-GNTI antagonized DPDPE-mediated inhibition of PGE_2-stimulated cAMP accumulation (Figure 5B, $F_{(1,42)} = 30.05$, $P < 0.0001$). The CRC for U50488 was not altered by DOR siRNA treatment (Figure 5A) nor was the CRC to DPDPE altered by KOR siRNA (Figure 5B).

DOR antagonists, NTI and BNTX, surmount occupancy of DOR by 6'-GNTI and block 6'-GNTI agonism ex vivo and in vivo

Results described above suggest that antagonist occupancy of DOR allosterically regulates KOR agonist potency and/or efficacy. We hypothesized that the mechanism that underlies 6'-GNTI agonist activity in peripheral nociceptors may be due to its occupancy of DOR producing positive allosteric regulation of its agonist efficacy at KOR within DOR-KOR heteromers. To test this hypothesis, we attempted first to surmount occupancy of DOR by 6'-GNTI using other DOR antagonists. As shown in Supplemental Figure 1, inhibition of cAMP accumulation by a maximal concentration of DPDPE (1 μM) was blocked by the DOR

Molecular Pharmacology Fast Forward. Published on February 7, 2018 as DOI: 10.1124/mol.117.109975
This article has not been copyedited and formatted. The final version may differ from this version.

antagonists, naltriben (NTB), NTI and BNTX, at concentrations of ~100 x Ki for DOR (Neilan et al., 1999; Raynor et al., 1994). As shown in Figure 6, both NTI and BNTX antagonized the effect of 6'-GNTI (Figure 6A and 6B, $F_{(1,42)}$ = 19.41, $P < 0.0001$ and $F_{(1,42)}$ = 19.91, $P < 0.0001$ for NTI and BNTX, respectively). By contrast, NTB did not alter the CRC to 6'-GNTI (Figure 6C; $F_{(1,42)}$ = 1.25, $P = 0.27$). The mean pEC_{50} for 6'-GNTI was 8.55 ± 0.23 (3 nM) and 8.83 ± 0.40 (1.5 nM) mean ± SEM, n=4, Veh and NTB, respectively, (paired t test, $P = 0.67$). The mean maximal inhibition of PGE_2-mediated stimulation of cAMP by 6'-GNTI was 52 ± 5% and 64 ± 10%, mean ± SEM, n=4, Veh and NTB, respectively (paired t test, $P = 0.10$).

In the behavioral model of thermal nociception, 6'-GNTI-mediated anti-allodynic responses were also antagonized by NTI ($F_{(1,62)}$, 10.39, $p = 0.002$; Figure 7A) and BNTX ($F_{(1,59)}$ = 13.37, $p = 0.0005$; Figure 7B). By contrast, NTB, at a dose that completely blocked maximal DPDPE-mediated antinociception (Supplemental Figure 3) did not alter the DRC of 6'-GNTI for reduction in PGE_2-mediated thermal allodynia (Figure 7C) ($F_{(1, 45)}$ =3.52, $P = 0.07$).

6'-GNTI-mediated anti-nociceptive signaling is blocked following disruption of DOR-KOR heteromers by a TAT-fused peptide corresponding to the TM1 domain of DOR

If the efficacy of 6'-GNTI is due to allosteric interactions between the DOR and KOR protomers of the heteromer, interference with the interaction between DOR and KOR would be expected to reduce the efficacy of 6'-GNTI. To test this, we treated peripheral sensory neurons ex vivo and in vivo with a TM peptide that corresponds to TM1 of DOR. We fused the TM1 peptide at its C-terminus with the cell-permeable HIV TAT sequence to confer membrane permeability and proper orientation of the TM domain within the membrane as described by He et al (2011). The TM1 domain is often implicated as a dimer interface of opioid receptors (e.g., (Gahbauer and Bockmann, 2016; He et al., 2011; Shang and Filizola, 2015). As a control, we

Molecular Pharmacology Fast Forward. Published on February 7, 2018 as DOI: 10.1124/mol.117.109975
This article has not been copyedited and formatted. The final version may differ from this version.

also tested a DOR TM1 peptide with the TAT sequence on the N-terminus (TAT-TM1 negative control), which would not insert into the membrane in the appropriate orientation.

As shown in Figure 8A, administration of the DOR TM1-TAT peptide did not alter the reduction of PGE_2-evoked thermal nociception by DPDPE or by U50488. However, the antinociceptive response to 6'-GNTI was abolished. By contrast, the DOR negative control TAT-TM1 peptide did not alter the antinociceptive response to 6'-GNTI (Figure 8B). Neither TAT-peptide altered BK- or PGE_2-evoked responses (Supplemental Figure 9A). In primary cultures of peripheral sensory neurons treated with DOR TM1-TAT, neither DPDPE- nor U50488-mediated inhibition of PGE_2-stimulated cAMP accumulation was altered (Figure 9A). However, 6'-GNTI-mediated inhibition of PGE_2-stimulated cAMP accumulation was eliminated completely. The TAT-TM1 negative control peptide did not alter the inhibition of AC activity by 6'-GNTI (Figure 9B).

Molecular Pharmacology Fast Forward. Published on February 7, 2018 as DOI: 10.1124/mol.117.109975
This article has not been copyedited and formatted. The final version may differ from this version.

Discussion

GPCR heteromers have been well studied in heterologous expression systems (Gomes et al., 2016), however, much less is known of heteromer function in physiologically relevant systems due, in large part, to methodological limitations and lack of available heteromer-selective ligands. However, it may be possible to exploit allosteric interactions that can occur between the protomers of a heteromer to study heteromer function in native systems. In this regard, orthosteric ligands binding to one protomer can act as allosteric regulators of the activity of orthosteric ligands that bind to the other protomer within a heteromer (Fuxe et al., 2010; Smith and Milligan, 2010). As a well-known hallmark of allosterism is that allosteric interactions are highly dependent upon the allosteric-orthosteric ligand pairs (Christopoulos et al., 2014; Kenakin, 2009; Smith and Milligan, 2010), it would be expected that inter-protomer allosteric effects of orthosteric ligands would be ligand-dependent as well.

Several studies have demonstrated allosteric interactions within DOR-KOR heteromers in heterologous expressions systems (Jordan and Devi, 1999; Waldhoer et al., 2005; Xie et al., 2005). In HEK cells co-expressing both DOR and KOR, but not in cells expressing either receptor alone, the affinity of the KOR agonist, U69593, is increased by the DOR agonist, DPDPE and, reciprocally, the affinity of DPDPE is increased by U69593 (Jordan and Devi, 1999). Allosteric interactions have also been reported for DOR and KOR antagonists (Xie et al., 2005).

In peripheral sensory neurons both ex vivo and in vivo, we have shown that KOR orthosteric antagonists alter DOR orthosteric agonist–mediated responses in a ligand-dependent manner (Berg et al., 2012). Here, we report that interactions between DOR and KOR orthosteric ligands in peripheral sensory neurons are reciprocal: DOR antagonists regulated KOR agonist-mediated responses and the nature of these effects was dependent on the DOR

Molecular Pharmacology Fast Forward. Published on February 7, 2018 as DOI: 10.1124/mol.117.109975
This article has not been copyedited and formatted. The final version may differ from this version.

antagonist/KOR agonist pair. For example, the DOR antagonist, NTI, had no effect on responses mediated by the KOR agonist, U50488, however it enhanced responses to the KOR agonist, ICI-199441 ex vivo and in vivo. Interestingly, the DOR-KOR heteromer selectivity of KDAN-18 (Daniels et al., 2005), which is composed of NTI and ICI-199441 linked together with an 18 carbon spacer, may be due to an allosteric effect of NTI via DOR to augment the KOR response to ICI-199441.

6'-GNTI is a guanidino derivative of the selective DOR antagonist, NTI. Addition of the guanidino group to the 5' position of NTI converts the compound to a KOR selective antagonist (5'-GNTI), whereas movement of the guanidino group to the 6′- position changes the ligand to a low efficacy KOR agonist (Rives et al., 2012; Schmid et al., 2013; Sharma et al., 2001). However, some studies have suggested that 6'-GNTI activates DOR-KOR heteromers (Ansonoff et al., 2010; Waldhoer et al., 2005). For example, 6'-GNTI has no efficacy at DOR and only weak efficacy at KOR when expressed individually in HEK cells, but when the receptors are co-expressed, the agonist efficacy of 6'-GNTI is greatly enhanced (Waldhoer et al., 2005). Although KOR is expressed in brain, 6'-GNTI had no effect when administered intracerebroventricularly. However when administered intrathecally, 6'-GNTI elicited antinociceptive responses that were blocked by either DOR or KOR antagonists (Waldhoer et al., 2005), or by knockout of either DOR or KOR (Ansonoff et al., 2010), indicating agonist efficacy in the spinal cord required both receptors. Consistent with these studies, we have shown previously that 6'-GNTI-mediated agonist responses in peripheral nociceptors are blocked by antagonists to either DOR or KOR (Berg et al., 2012) and in the present study, we found that siRNA knock-down of either DOR or KOR expression blocked 6'-GNTI-mediated inhibition of adenylyl cyclase activity in cultured peripheral sensory neurons. Moreover, when DOR expression was reduced, 6'-GNTI did not activate KOR, but instead behaved as an antagonist. These data suggest that, compared to high expression that can occur in

Molecular Pharmacology Fast Forward. Published on February 7, 2018 as DOI: 10.1124/mol.117.109975
This article has not been copyedited and formatted. The final version may differ from this version.

heterologous systems, KOR expression in brain, spinal cord, and peripheral sensory neurons is too low for the low efficacy of 6'-GNTI to be observed, however, in the presence of DOR, 6'-GNTI efficacy is increased.

Given that efficacy of 6'-GNTI in peripheral sensory neurons ex vivo and in vivo is dependent upon DOR and KOR, that 6'-GNTI bound to both DOR and KOR, and that some orthosteric DOR antagonists could enhance KOR agonist responses, we considered that perhaps the efficacy of 6'-GNTI was due to positive allosteric augmentation of efficacy at KOR by its occupancy of DOR. Using siRNA knock-down of KOR, we found that 6'-GNTI functioned as a DOR antagonist, consistent with having affinity but no efficacy at DOR as reported by Waldhoer et al. (2005). Furthermore, when the occupancy of 6'-GNTI of DOR was surmounted with other DOR antagonists, NTI and BNTX, the agonist activity of 6'-GNTI was reduced both ex vivo and in vivo. By contrast, NTB substituted for 6'-GNTI at DOR, as 6'-GNTI-mediated responses ex vivo and in vivo were not altered. The differential effects of DOR antagonists on 6'-GNTI responsiveness support the hypothesis that, in peripheral nociceptors, 6'-GNTI allosterically regulates its own agonist efficacy at KOR via occupancy of DOR. We suggest that this mechanism provides for selectivity of 6'-GNTI for DOR-KOR heteromers in peripheral sensory neurons and perhaps other areas, such as spinal cord.

If the DOR-dependent effect of 6'-GNTI to augment efficacy at KOR is via allosteric interactions between the DOR and KOR protomers of DOR-KOR heteromers, then approaches that interfere with interactions between DOR and KOR should also interfere with the efficacy of 6'-GNTI. To test this hypothesis, we measured the efficacy of 6'-GNTI following delivery of peptides that correspond to the TM1 domain of DOR to peripheral sensory neurons ex vivo and in vivo. Following the method reported by He et al. (2011), DOR TM1 domain peptides were fused to the HIV TAT sequence to increase membrane permeability. Administration of DOR TM1 peptides, with the TAT sequence fused to the C-terminus completely prevented efficacy of

Molecular Pharmacology Fast Forward. Published on February 7, 2018 as DOI: 10.1124/mol.117.109975
This article has not been copyedited and formatted. The final version may differ from this version.

6'-GNTI both for inhibition of adenylyl cyclase activity in peripheral sensory neurons in culture and for inhibition of thermal allodynia in behavioral tests. Control peptides with the TAT sequence fused to the N-terminus, which would be expected to orient the TM1 sequence in the opposite direction in the membrane, were ineffective. Taken together, these results suggest that the efficacy of 6'-GNTI is due to intra-heteromer allosteric interactions between DOR occupied by 6'-GNTI and KOR occupied by 6'-GNTI. Furthermore, these results suggest that in peripheral sensory neurons, 6'-GNTI selectively activates DOR-KOR heteromers.

Interestingly, efficacy of 6'-GNTI appears to be cell/tissue specific. In this regard, Kenakin showed over 30 years ago that the selective β1-adrenergic receptor ligand, prenalterol, is either a full agonist, a partial agonist or an antagonist (i.e., has no efficacy) depending upon the tissue studied (Kenakin and Beek, 1980). Similarly, 6'-GNTI has been shown to have KOR agonist activity in some cells/tissues, but antagonist activity in others. In guinea pig ileum, 6'-GNTI inhibits electrically-stimulated smooth muscle contraction via KOR, but is inactive in smooth muscle preparations from mouse vas deferens (Sharma et al., 2001). In KOR expressing HEK cells, 6'-GNTI is a partial agonist for inhibition of adenylyl cyclase activity and its efficacy is not altered by co-expression of DOR (Rives et al., 2012). In CHO cells expressing KOR, but not in striatal neurons endogenously expressing KOR, 6'-GNTI is an agonist for activation of Gαi using the GTPγS assay (Schmid et al., 2013). Interestingly, although 6'-GNTI did not increase GTPγS binding in striatal neurons, it did activate Akt in a pertussis toxin-dependent and ß-arrestin-independent manner. This latter finding highlights the importance of the sensitivity of the assay used to assess ligand efficacy. In our experiments, although 6'-GNTI could bind to both DOR and KOR, efficacy of 6'-GNTI for antinociception or to inhibit adenylyl cyclase activity required both DOR and KOR. Taken together, it is likely that 6'-GNTI is a low efficacy agonist at KOR for activation of Gαi signaling. Depending upon the density of KOR expression (high in heterologous expression systems) and on the strength of receptor-effector

coupling efficiency (e.g. the quantity and perhaps type of Gαi and accessory proteins expressed), a weak KOR activating signal of 6'-GNTI may be amplified to a level where agonism is observed. However, in cells/tissues where KOR expression is low (as is typical of receptors expressed in native systems), or receptor-effector coupling is weak, 6'-GNTI may behave as a KOR antagonist, as we have found in peripheral sensory neurons.

In summary, in both ex vivo and in vivo models of peripheral sensory neuron function, DOR antagonists differentially regulated KOR agonist responses in a ligand-dependent manner. Taken together with our previous findings (Berg et al., 2012), these results support the existence of functional DOR-KOR heteromers in rat peripheral sensory neurons and are consistent with the notion that reciprocal, ligand-dependent, allosteric interactions occur between the DOR and KOR protomers. Because its probable that homomers/monomers are expressed, we have likely underestimated the magnitude of the allosteric effects. Given the limitations of tools to study GPCR heteromer function in physiologically-relevant systems and the paucity of selective ligands, perhaps capitalizing on allosteric effects of orthosteric ligands selective for the individual protomers may provide a viable approach to study heteromer function in native systems.

Molecular Pharmacology Fast Forward. Published on February 7, 2018 as DOI: 10.1124/mol.117.109975
This article has not been copyedited and formatted. The final version may differ from this version.

Acknowledgements

We would like to thank Hudson Smith and Joshua Zamora for excellent technical assistance and Drs. Lakshmi Devi and Milena Girotti for helpful discussions.

Authorship Contributions:

Participated in research design: Jacobs, Pando, Berg and Clarke

Conducted experiments: Jacobs, Chavera, Jennings and Pando

Performed data analysis: Jacobs, Berg, Jennings and Pando

Wrote or contributed to the writing of the manuscript: Jacobs, Berg and Clarke

References

Ansonoff MA, Portoghese PS and Pintar JE (2010) Consequences of opioid receptor mutation on actions of univalent and bivalent kappa and delta ligands. *Psychopharmacology (Berl)* **210**(2):161-168.

Berg KA, Patwardhan AM, Sanchez TA, Silva YM, Hargreaves KM and Clarke WP (2007) Rapid modulation of mu-opioid receptor signaling in primary sensory neurons. *J Pharmacol Exp Ther* **321**(3):839-847.

Berg KA, Rowan MP, Gupta A, Sanchez TA, Silva M, Gomes I, McGuire BA, Portoghese PS, Hargreaves KM, Devi LA and Clarke WP (2012) Allosteric Interactions between delta and kappa opioid receptors in peripheral sensory neurons. *Mol Pharmacol* **81**(2):264-272.

Berg KA, Rowan MP, Sanchez TA, Silva M, Patwardhan AM, Milam SB, Hargreaves KM and Clarke WP (2011) Regulation of kappa-opioid receptor signaling in peripheral sensory neurons in vitro and in vivo. *J Pharmacol Exp Ther* **338**(1):92-99.

Brooks H, Lebleu B and Vives E (2005) Tat peptide-mediated cellular delivery: back to basics. *Adv Drug Deliv Rev* **57**(4):559-577.

Charles AC, Mostovskaya N, Asas K, Evans CJ, Dankovich ML and Hales TG (2003) Coexpression of delta-opioid receptors with micro receptors in GH3 cells changes the functional response to micro agonists from inhibitory to excitatory. *Mol Pharmacol* **63**(1):89-95.

Christopoulos A, Changeux JP, Catterall WA, Fabbro D, Burris TP, Cidlowski JA, Olsen RW, Peters JA, Neubig RR, Pin JP, Sexton PM, Kenakin TP, Ehlert FJ, Spedding M and

Langmead CJ (2014) International Union of Basic and Clinical Pharmacology. XC. multisite pharmacology: recommendations for the nomenclature of receptor allosterism and allosteric ligands. *Pharmacol Rev* **66**(4):918-947.

Clark MJ, Emmerson PJ, Mansour A, Akil H, Woods JH, Portoghese PS, Remmers AE and Medzihradsky F (1997) Opioid efficacy in a C6 glioma cell line stably expressing the delta opioid receptor. *J Pharmacol Exp Ther* **283**(2):501-510.

Daniels DJ, Kulkarni A, Xie Z, Bhushan RG and Portoghese PS (2005) A bivalent ligand (KDAN-18) containing delta-antagonist and kappa-agonist pharmacophores bridges delta2 and kappa1 opioid receptor phenotypes. *J Med Chem* **48**(6):1713-1716.

Ellis J, Pediani JD, Canals M, Milasta S and Milligan G (2006) Orexin-1 receptor-cannabinoid CB1 receptor heterodimerization results in both ligand-dependent and -independent coordinated alterations of receptor localization and function. *J Biol Chem* **281**(50):38812-38824.

Ferre S, Bonaventura J, Tomasi D, Navarro G, Moreno E, Cortes A, Lluis C, Casado V and Volkow ND (2016) Allosteric mechanisms within the adenosine A2A-dopamine D2 receptor heterotetramer. *Neuropharmacology* **104**:154-160.

Fuxe K, Marcellino D, Borroto-Escuela DO, Frankowska M, Ferraro L, Guidolin D, Ciruela F and Agnati LF (2010) The changing world of G protein-coupled receptors: from monomers to dimers and receptor mosaics with allosteric receptor-receptor interactions. *J Recept Signal Transduct Res* **30**(5):272-283.

Gahbauer S and Bockmann RA (2016) Membrane-Mediated Oligomerization of G Protein Coupled Receptors and Its Implications for GPCR Function. *Front Physiol* **7**:494.

Gomes I, Ayoub MA, Fujita W, Jaeger WC, Pfleger KD and Devi LA (2016) G Protein-Coupled Receptor Heteromers. *Annu Rev Pharmacol Toxicol* **56**:403-425.

Guitart X, Navarro G, Moreno E, Yano H, Cai NS, Sanchez-Soto M, Kumar-Barodia S, Naidu YT, Mallol J, Cortes A, Lluis C, Canela EI, Casado V, McCormick PJ and Ferre S (2014) Functional selectivity of allosteric interactions within G protein-coupled receptor oligomers: the dopamine D1-D3 receptor heterotetramer. *Mol Pharmacol* **86**(4):417-429.

Hargreaves K, Dubner R, Brown F, Flores C and Joris J (1988) A new and sensitive method for measuring thermal nociception in cutaneous hyperalgesia. *Pain* **32**(1):77-88.

He SQ, Zhang ZN, Guan JS, Liu HR, Zhao B, Wang HB, Li Q, Yang H, Luo J, Li ZY, Wang Q, Lu YJ, Bao L and Zhang X (2011) Facilitation of mu-opioid receptor activity by preventing delta-opioid receptor-mediated codegradation. *Neuron* **69**(1):120-131.

Jamshidi RJ, Jacobs BA, Sullivan LC, Chavera TA, Saylor RM, Prisinzano TE, Clarke WP and Berg KA (2015) Functional selectivity of kappa opioid receptor agonists in peripheral sensory neurons. *J Pharmacol Exp Ther* **355**(2):174-182.

Jordan BA and Devi LA (1999) G-protein-coupled receptor heterodimerization modulates receptor function. *Nature* **399**(6737):697-700.

Kenakin TP (2009) '7TM receptor allostery: putting numbers to shapeshifting proteins. *Trends Pharmacol Sci* **30**(9):460-469.

Kenakin TP and Beek D (1980) Is prenalterol (H133/80) really a selective beta 1 adrenoceptor agonist? Tissue selectivity resulting from differences in stimulus-response relationships. *J Pharmacol Exp Ther* **213**(2):406-413.

Martin NA and Prather PL (2001) Interaction of co-expressed mu- and delta-opioid receptors in transfected rat pituitary GH(3) cells. *Mol Pharmacol* **59**(4):774-783.

Neilan CL, Akil H, Woods JH and Traynor JR (1999) Constitutive activity of the delta-opioid receptor expressed in C6 glioma cells: identification of non-peptide delta-inverse agonists. *Br J Pharmacol* **128**(3):556-562.

Raynor K, Kong H, Chen Y, Yasuda K, Yu L, Bell GI and Reisine T (1994) Pharmacological characterization of the cloned kappa-, delta-, and mu-opioid receptors. *Mol Pharmacol* **45**(2):330-334.

Rives ML, Rossillo M, Liu-Chen LY and Javitch JA (2012) 6'-Guanidinonaltrindole (6'-GNTI) is a G protein-biased kappa-opioid receptor agonist that inhibits arrestin recruitment. *J Biol Chem* **287**(32):27050-27054.

Rowan MP, Ruparel NB, Patwardhan AM, Berg KA, Clarke WP and Hargreaves KM (2009) Peripheral delta opioid receptors require priming for functional competence in vivo. *Eur J Pharmacol* **602**(2-3):283-287.

Rozenfeld R, Bushlin I, Gomes I, Tzavaras N, Gupta A, Neves S, Battini L, Gusella GL, Lachmann A, Ma'ayan A, Blitzer RD and Devi LA (2012) Receptor heteromerization expands the repertoire of cannabinoid signaling in rodent neurons. *PLoS One* **7**(1):e29239.

Schmid CL, Streicher JM, Groer CE, Munro TA, Zhou L and Bohn LM (2013) Functional selectivity of 6'-guanidinonaltrindole (6'-GNTI) at kappa-opioid receptors in striatal neurons. *J Biol Chem* **288**(31):22387-22398.

Shang Y and Filizola M (2015) Opioid receptors: Structural and mechanistic insights into pharmacology and signaling. *Eur J Pharmacol* **763**(Pt B):206-213.

Sharma SK, Jones RM, Metzger TG, Ferguson DM and Portoghese PS (2001) Transformation of a kappa-opioid receptor antagonist to a kappa-agonist by transfer of a guanidinium group from the 5'- to 6'-position of naltrindole. *J Med Chem* **44**(13):2073-2079.

Shivnaraine RV, Kelly B, Sankar KS, Redka DS, Han YR, Huang F, Elmslie G, Pinto D, Li Y, Rocheleau JV, Gradinaru CC, Ellis J and Wells JW (2016) Allosteric modulation in monomers and oligomers of a G protein-coupled receptor. *Elife* **5** pii: e11685.

Siddiquee K, Hampton J, McAnally D, May L and Smith L (2013) The apelin receptor inhibits the angiotensin II type 1 receptor via allosteric trans-inhibition. *Br J Pharmacol* **168**(5):1104-1117.

Smith NJ and Milligan G (2010) Allostery at G protein-coupled receptor homo- and heteromers: uncharted pharmacological landscapes. *Pharmacol Rev* **62**(4):701-725.

Stein C and Lang LJ (2009) Peripheral mechanisms of opioid analgesia. *Curr Opin Pharmacol* **9**(1):3-8.

Stein C and Zollner C (2009) Opioids and sensory nerves. *Handb Exp Pharmacol*(194):495-518.

Sullivan LC, Berg KA and Clarke WP (2015) Dual regulation of delta-opioid receptor function by arachidonic acid metabolites in rat peripheral sensory neurons. *J Pharmacol Exp Ther* **353**(1):44-51.

Vischer HF, Watts AO, Nijmeijer S and Leurs R (2011) G protein-coupled receptors: walking hand-in-hand, talking hand-in-hand? *Br J Pharmacol* **163**(2):246-260.

Waldhoer M, Fong J, Jones RM, Lunzer MM, Sharma SK, Kostenis E, Portoghese PS and Whistler JL (2005) A heterodimer-selective agonist shows in vivo relevance of G protein-coupled receptor dimers. *Proc Natl Acad Sci U S A* **102**(25):9050-9055.

Wang D, Sun X, Bohn LM and Sadee W (2005) Opioid receptor homo- and heterodimerization in living cells by quantitative bioluminescence resonance energy transfer. *Mol Pharmacol* **67**(6):2173-2184.

Xie Z, Bhushan RG, Daniels DJ and Portoghese PS (2005) Interaction of bivalent ligand KDN21 with heterodimeric delta-kappa opioid receptors in human embryonic kidney 293 cells. *Mol Pharmacol* **68**(4):1079-1086.

Footnotes:

This work was supported by US Public Health Service grants from the National Institutes of Health: [R01 GM 106035] and [R21 DA 037572] to WPC and KAB; the National Institute of Dental and Craniofacial Research (COSTAR) Training Grant [T32DE14318]) to BAJ; and the National Institute on Neurological Disorders and Stroke Training Grant [T32 NS 082145] to MMP.

Molecular Pharmacology Fast Forward. Published on February 7, 2018 as DOI: 10.1124/mol.117.109975
This article has not been copyedited and formatted. The final version may differ from this version.

Figure Legends

Figure 1. Ligand-dependent effects of the DOR antagonist, naltrindole (NTI) on concentration response curves for the KOR agonists, ICI-199441 (A) and U50488 (B) for inhibition of PGE_2-stimulated cAMP accumulation. Primary cultures of peripheral sensory neurons were pretreated with NTI (20 nM) or vehicle (Veh) for 15 min. Following pretreatment, cells were treated with various concentrations of ICI-199441 or U50488, along with PGE_2 (1 μM) and the phosphodiesterase inhibitor, rolipram. Cellular cAMP levels were measured after 15 min. Data are expressed as the percentage of PGE_2-stimulated cAMP levels and represent the mean ± S.E.M (n=5). In the presence of NTI, the curve to ICI-199441 **(A)** was shifted to the left ($F_{(1,56)}$ = 21.65, P < 0.0001). By contrast, NTI did not alter the curve to U50488 (**B**; $F_{(1,56)}$ = 0.217, P = 0.64) (**A)** Basal cAMP levels were 0.51 ± .07 pmol/well vs. 0.45 ± 0.07 pmol/well, Veh and NTI, respectively and PGE_2–stimulated cAMP levels were 217% ± 45% above basal and 241% ± 22% above basal Veh and NTI, respectively (mean ± SEM, n=5). **(B)** Basal cAMP levels were 0.80 ± 0.16 pmol/well vs. 0.91 ± 0.19 pmol/well, Veh and NTI, respectively and PGE_2–stimulated cAMP levels were 186% ± 33% above basal and 130% ± 26% above basal, Veh and NTI, respectively (mean ± SEM, n=5). As shown in Supplemental Figure 1, NTI (20 nM) completely antagonized a maximal concentration of DPDPE (100 nM) for inhibition of cAMP accumulation, indicating full occupancy of DOR at this concentration.

Figure 2. Ligand-dependent effects of the DOR antagonist, naltrindole (NTI) on dose response curves for the KOR agonists, ICI-199441 (A) and U50488 (B) for inhibition of PGE_2-stimulated thermal allodynia. Rats received intraplantar injection of NTI (40 μg) 15 min before intraplantar injection of PGE_2 (0.3 μg) along with either ICI-199441 or U50488 at the indicated doses. Data are expressed as the change in seconds (s) from individual baseline pre-

Molecular Pharmacology Fast Forward. Published on February 7, 2018 as DOI: 10.1124/mol.117.109975
This article has not been copyedited and formatted. The final version may differ from this version.

injection values 10-min post PGE_2 ± opioid agonist administration and represent mean ± SEM of 6-9 animals per group. In the presence of NTI, the ICI-199441 curve was shifted significantly to the left ($F_{(1,75)}$ = 9.849; P = 0.0024). By contrast, the curve for U50488 was not altered by NTI ($F_{(1,59)}$ = .8098; P = 0.37). Injection of NTI alone had no effect on baseline PWL ($F(_{1,40)}$ = 1.299, P = 0.27) or on PGE_2–evoked thermal allodynia ($F_{(1,52)}$ = 0.109; P = 0.74). As shown in Supplemental Figure 3, injection of 40 µg NTI completely blocked a maximal dose of DPDPE for inhibition of PGE_2-induced thermal nociception. Full time course curves are presented in Supplemental Figures 4 and 5.

Figure 3. The DOR antagonist, BNTX, increases the potency of U50488 for reduction of PGE_2-evoked thermal allodynia and the BNTX effect is blocked by NTI. Rats were injected (i.pl.) with BK (25 µg) in combination with vehicle (Veh), BNTX (1µg) or NTI (40 µg) plus BNTX (1 µg) 15 min before intraplantar injection with PGE_2 (0.3 µg) with our without U50488 at the indicated doses. Paw withdrawal latencies are expressed as the change (seconds) from individual baseline values 10-min post PGE_2/U50488 administration and represent mean ± SEM of 6-12 animals per group. Data were analyzed for statistical significance using two-way ANOVA. The U50488 curve in the presence of BNTX was significantly different from Veh, ($F_{(1, 121)}$ = 4.08, P= 0.04). By contrast, the U50488 curve in the presence of BNTX and NTI in combination was not different from Veh, ($F_{(1, 89)}$ = 3.177, P = 0.08). Full time course curves are presented in Supplemental Figure 6.

Figure 4. 6'-GNTI agonist efficacy requires occupancy of both DOR and KOR in peripheral sensory neurons. Primary cultures of peripheral sensory neurons were transfected with siRNA directed against DOR (gray), KOR (white), or non-targeting siRNA as a control (black). Five days after transfection, inhibition of PGE_2-stimulated cAMP accumulation in

Molecular Pharmacology Fast Forward. Published on February 7, 2018 as DOI: 10.1124/mol.117.109975
This article has not been copyedited and formatted. The final version may differ from this version.

response to **(A)** U50488 (100 nM), **(B)** DPDPE (100 nM), **(C)** DAMGO (100 nM), or **(D)** 6'-GNTI (100 nM) was measured. Data are expressed as the percentage of PGE_2-stimulated cAMP levels and are the mean ± SEM, n=6. ***P < 0.001, ****P < 0.0001 vs. off-target (control) siRNA, one-way ANOVA with Dunnett's post test.

Figure 5. Antagonism of responses to U50488 (A) and DPDPE (B) by 6'-GNTI following knockdown of DOR (A) or KOR (B) in peripheral sensory neurons. Primary cultures of peripheral sensory neurons were transfected with or without siRNA directed against either DOR **(A)** or KOR **(B)**. Five days after transfection, cells were treated with PGE_2 (1 μM) along with various concentrations of U50288 **(A)** or DPDPE **(B)** with 6'-GNTI (1 μM) or vehicle (Veh). Data are expressed as the percentage of PGE_2-stimulated cAMP levels and are the mean ± SEM, n=4. Data were analyzed for statistical significance using two-way ANOVA. In cells treated with DOR siRNA **(A)**, the U50488 curve in the presence 6'-GNTI was significantly different from Veh, ($F_{(1,42)}$ = 44.23, P < 0.0001). In cells treated with KOR siRNA **(B)**, the U50488 curve in the presence 6'-GNTI was significantly different from Veh, ($F_{(1,42)}$ = 30.05, P < 0.0001).

Figure 6. Differential effects of DOR occupancy with selective antagonists on 6'-GNTI-mediated inhibition of PGE_2-stimulated cAMP accumulation ex vivo. Primary cultures of peripheral sensory neurons were pretreated with vehicle (Veh), NTI (20 nM) **(A)** BNTX (200 nM) **(B)** or NTB (1 nM) **(C)** for 15 min. After pretreatment, cells were incubated for 15 min with PGE_2 with or without the indicated concentrations of 6'-GNTI. Data are expressed as the percentage of PGE_2-stimulated cAMP levels and are the mean ± SEM, n=4 separate experiments. Data were analyzed for statistical significance using two-way ANOVA. The 6'-GNTI curve in the presence of NTI **(A)** and BNTX **(B)** was significantly different from Veh, ($F_{(1,42)}$ = 19.41, P <

Molecular Pharmacology Fast Forward. Published on February 7, 2018 as DOI: 10.1124/mol.117.109975
This article has not been copyedited and formatted. The final version may differ from this version.

0.0001 and $F_{(1,42)}$ = 19.91, $P < 0.0001$ for NTI and BNTX, respectively). By contrast, the 6'-GNTI curve in the presence of NTB **(C)** was not different from Veh, ($F_{1,42)}$ = 1.25, P = 0.269). Incubation with antagonists did not alter either basal cAMP levels or PGE_2-stimulated cAMP levels which were 1.34 pmol/well ± 0.23 and 220% above basal ± 47%, mean ± SEM, n=12.

Figure 7. Differential effects of DOR occupancy with selective antagonists on 6'-GNTI-mediated antinociception. Rats received intraplantar injection with either NTI (40 µg) **(A)** BNTX (1 µg) (**B)** or NTB (1 µg) **(C)** 15 min before intraplantar injection with PGE_2 (0.3 µg) in combination with either Veh or the indicated doses of 6'-GNTI. Data are expressed as the change (seconds) from individual preinjection baseline values 10-min post PGE_2 ± 6'-GNTI injection and represent mean ± SEM of 6-12 animals per group. Data were analyzed for statistical significance using two-way ANOVA. The 6'-GNTI curve in the presence of NTI **(A)** or BNTX **(B)** was significantly different from Veh ($F_{(1,62)}$ = 10.39, p = 0.002 and $F_{(1,59)}$ = 13.37, p = 0.0005, for NTI and BNTX, respectively). NTB **(C)** did not alter the 6'-GNTI curve ($F_{(1, 45)}$ = 3.52, P = 0.07). As shown in Supplemental Figure 3, none of the DOR antagonists altered baseline PWLs or PGE_2–induced thermal allodynia. Full timecourse curves are shown in Supplemental Figure 8.

Figure 8. 6'-GNTI-mediated antinociception is blocked following disruption of DOR-KOR heteromers by DOR TM1-TAT peptides. Rats received an injection of either vehicle, DOR-TM1-TAT peptide (3.94 µg, i.pl.) **(A)** or TM-TAT negative control peptide (3.94 µg, i.pl.) **(B)** followed 30 min later with a co-injection of PGE_2 (0.3 µg) with vehicle, DPDPE (20 µg i.pl.), U50488 (0.1 µg i.pl.) or 6'-GNTI (1 µg, i.pl.). Data are expressed as the change (seconds) from individual preinjection baseline values 10-min post PGE_2 + agonist injection and represent mean

Molecular Pharmacology Fast Forward. Published on February 7, 2018 as DOI: 10.1124/mol.117.109975
This article has not been copyedited and formatted. The final version may differ from this version.

± SEM of 6 animals per group. Data were analyzed for statistical differences with one-way ANOVA followed by Bonferroni's post test, ****, $p < 0.0001$. Full timecourse curves are shown in Supplemental Figure 9.

Figure 9. 6'-GNTI-mediated inhibition of PGE_2-stimulated cAMP accumulation is blocked following disruption of DOR-KOR heteromers by DOR TM1-TAT peptides. Primary cultures of peripheral sensory neurons were treated with vehicle, the DOR TM1-TAT peptide (1 μM) **(A)** or with the negative control TAT-TM1 peptide (1 μM) **(B)** for 30 min. Cells were incubated with PGE_2 (1 μM) and either Veh, 6'-GNTI (100 nM), DPDPE (100 nM) or U50488 (100 nM) for an additional 15 min. Data are expressed as the percentage of PGE_2-stimulated cAMP levels and are the mean ± SEM, n=4. ****$P < 0.0001$ vs. vehicle (no TM peptide), one-way ANOVA with Dunnett's post test.

Molecular Pharmacology Fast Forward. Published on February 7, 2018 as DOI: 10.1124/mol.117.109975
This article has not been copyedited and formatted. The final version may differ from this version.

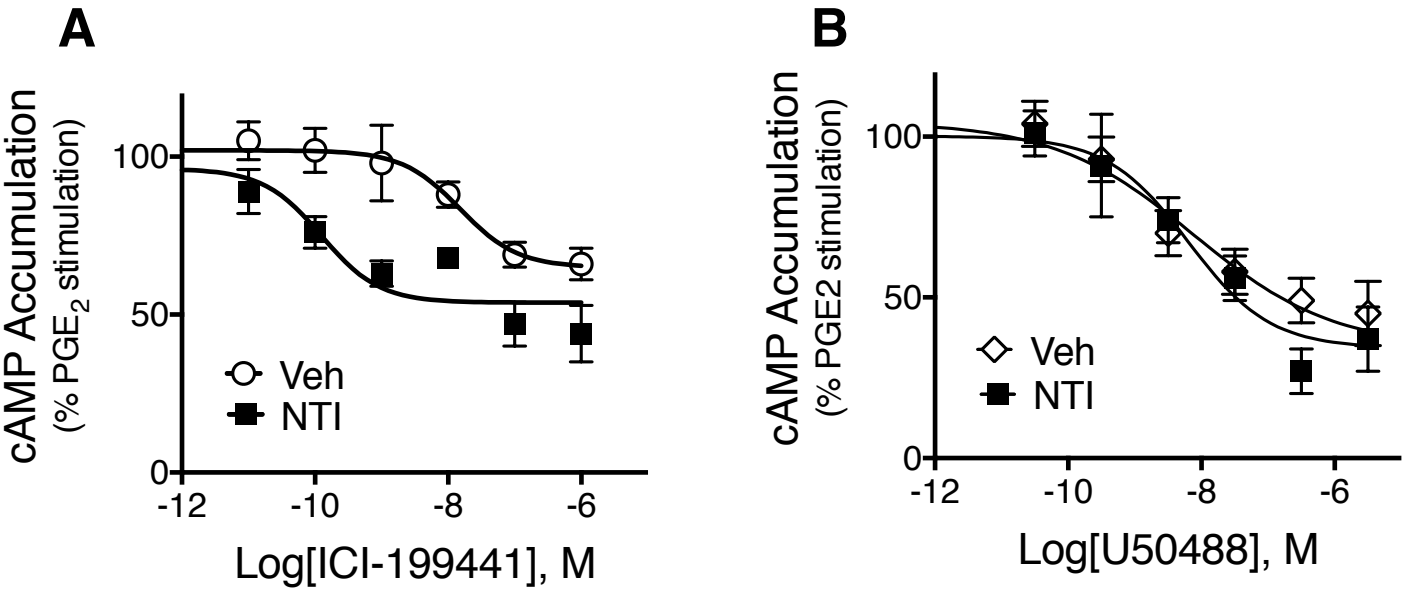

Figure 1

Molecular Pharmacology Fast Forward. Published on February 7, 2018 as DOI: 10.1124/mol.117.109975
This article has not been copyedited and formatted. The final version may differ from this version.

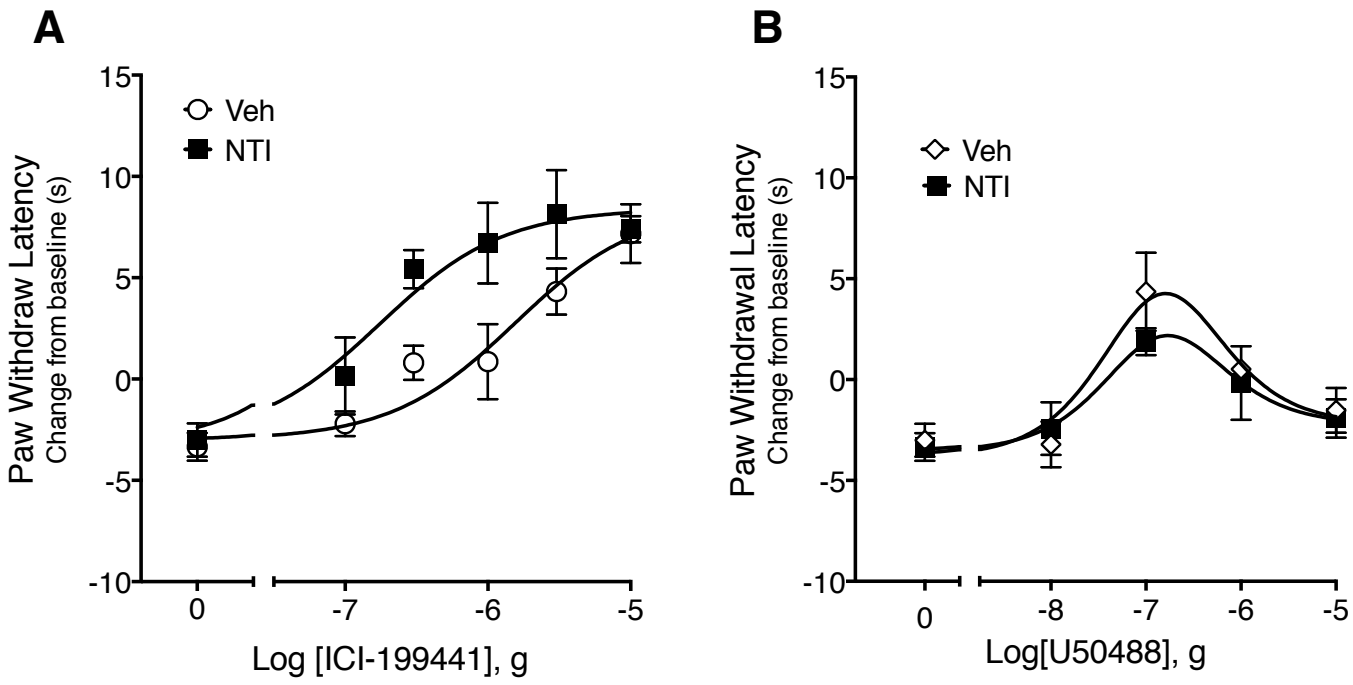

Figure 2

Molecular Pharmacology Fast Forward. Published on February 7, 2018 as DOI: 10.1124/mol.117.109975
This article has not been copyedited and formatted. The final version may differ from this version.

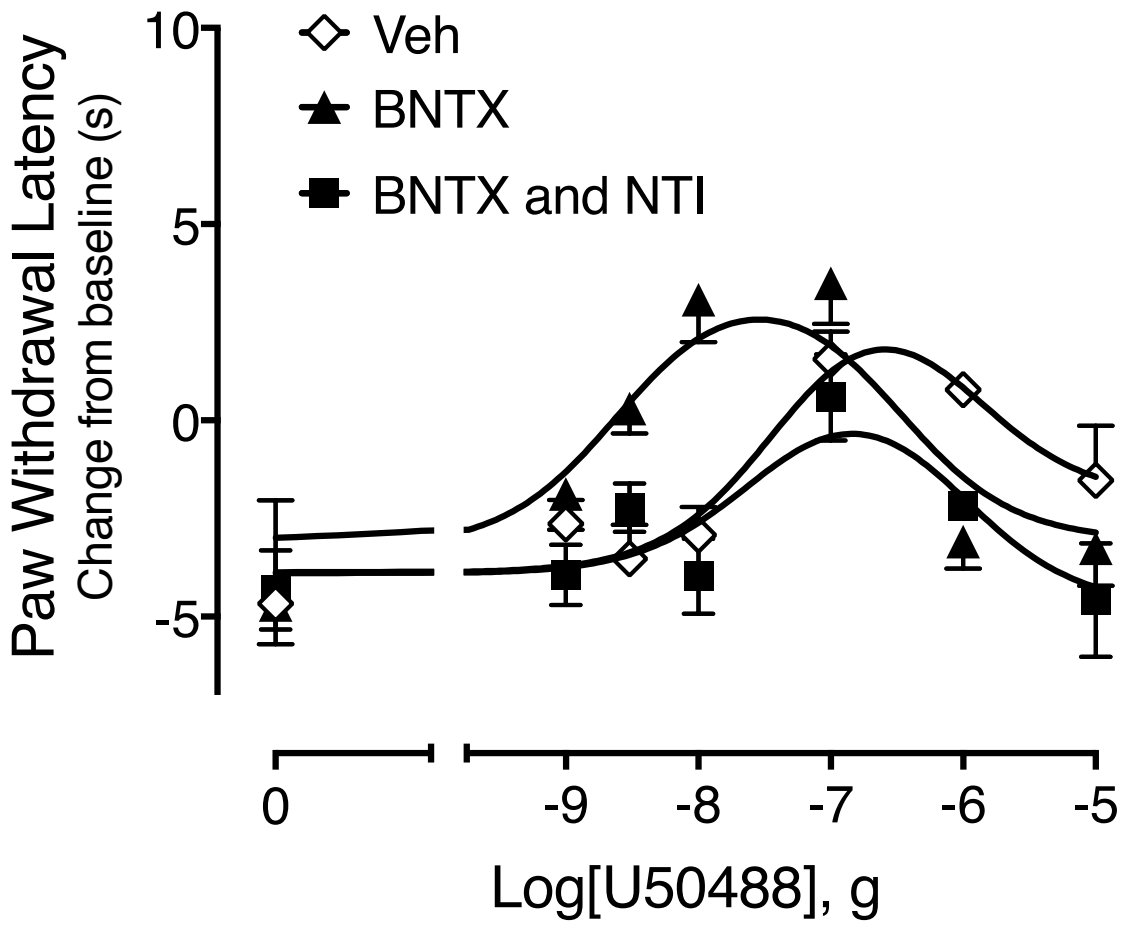

Figure 3

Molecular Pharmacology Fast Forward. Published on February 7, 2018 as DOI: 10.1124/mol.117.109975
This article has not been copyedited and formatted. The final version may differ from this version.

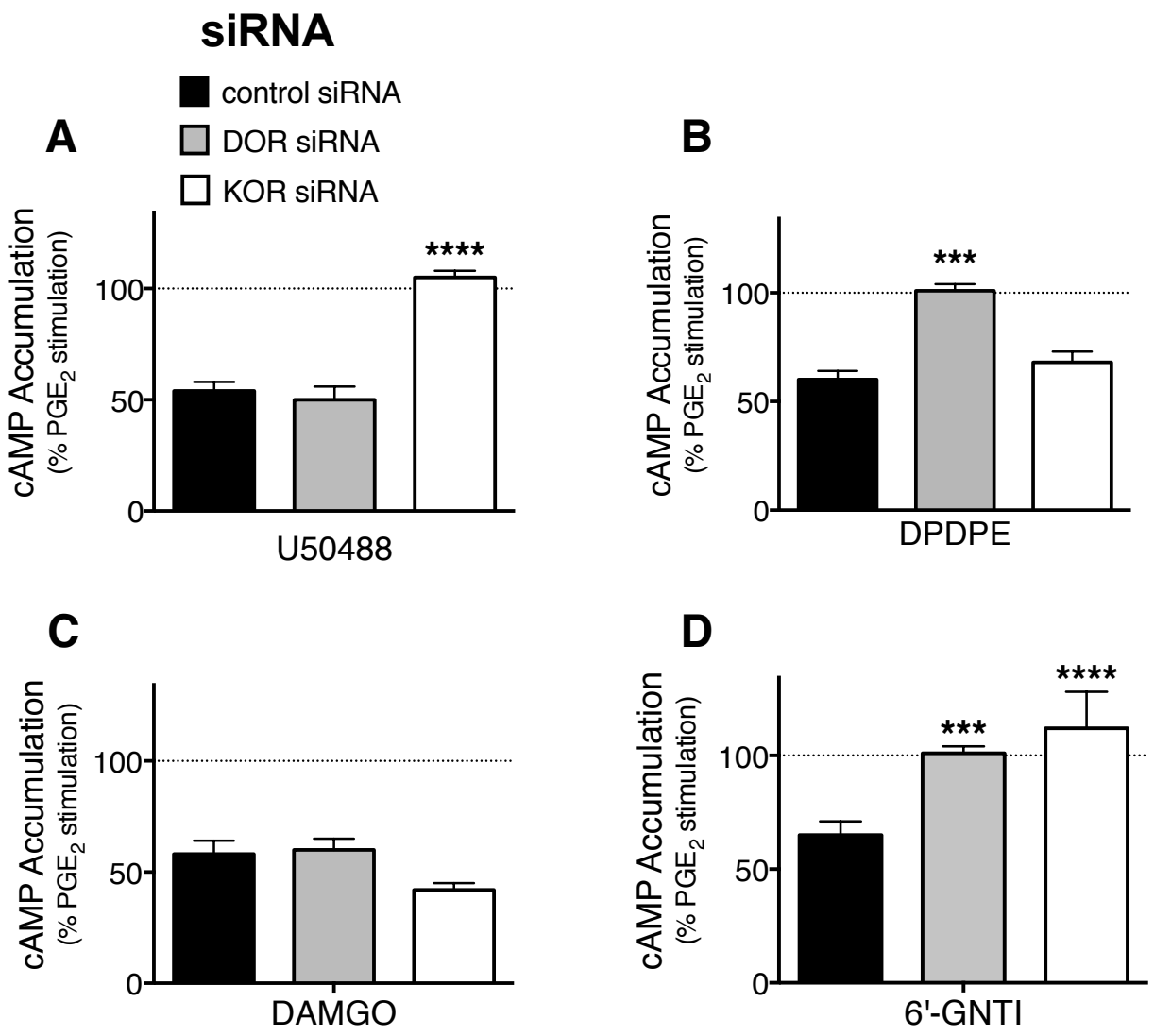

Figure 4

Molecular Pharmacology Fast Forward. Published on February 7, 2018 as DOI: 10.1124/mol.117.109975
This article has not been copyedited and formatted. The final version may differ from this version.

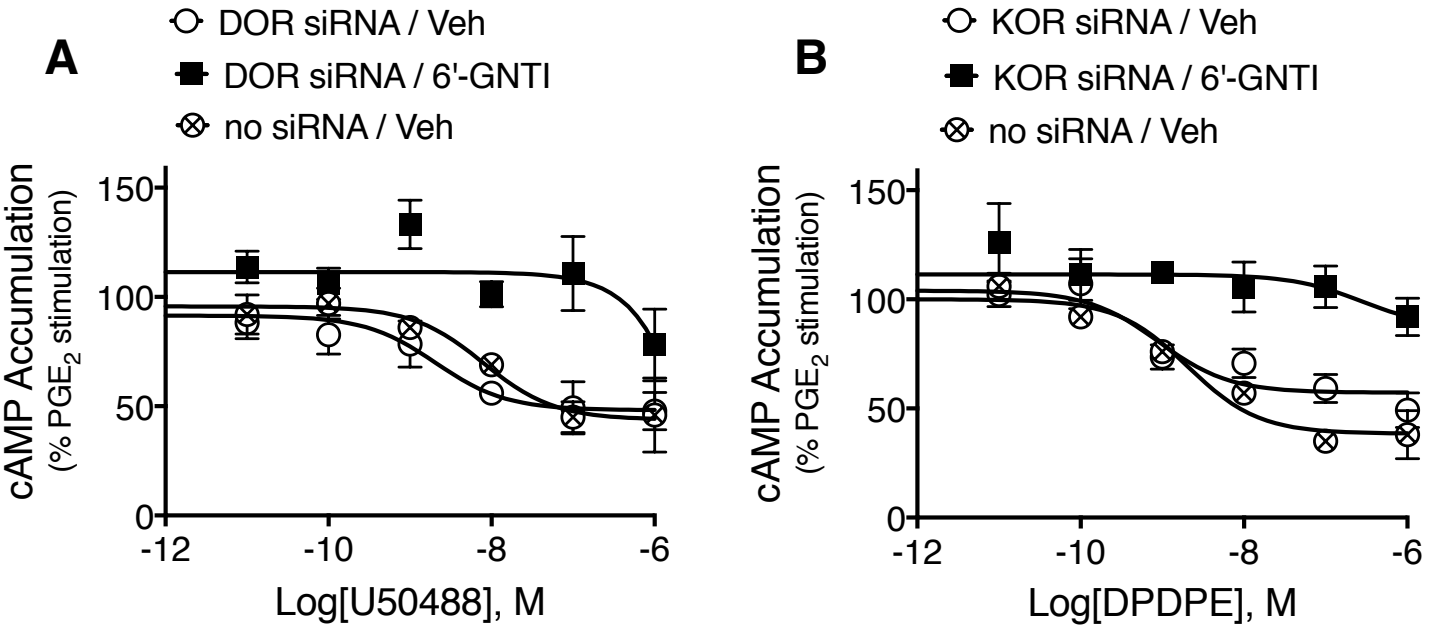

Figure 5

Molecular Pharmacology Fast Forward. Published on February 7, 2018 as DOI: 10.1124/mol.117.109975
This article has not been copyedited and formatted. The final version may differ from this version.

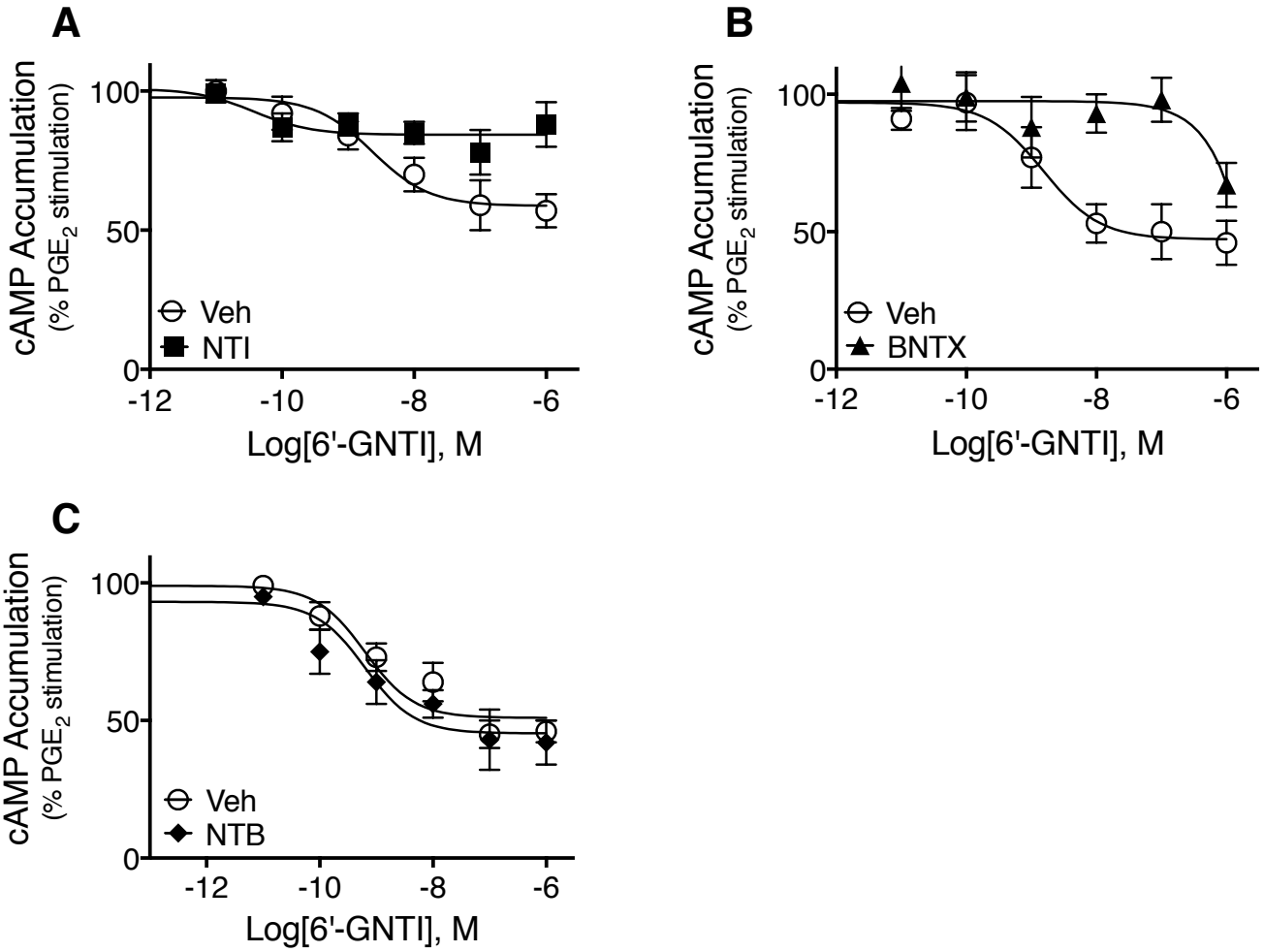

Figure 6

Molecular Pharmacology Fast Forward. Published on February 7, 2018 as DOI: 10.1124/mol.117.109975
This article has not been copyedited and formatted. The final version may differ from this version.

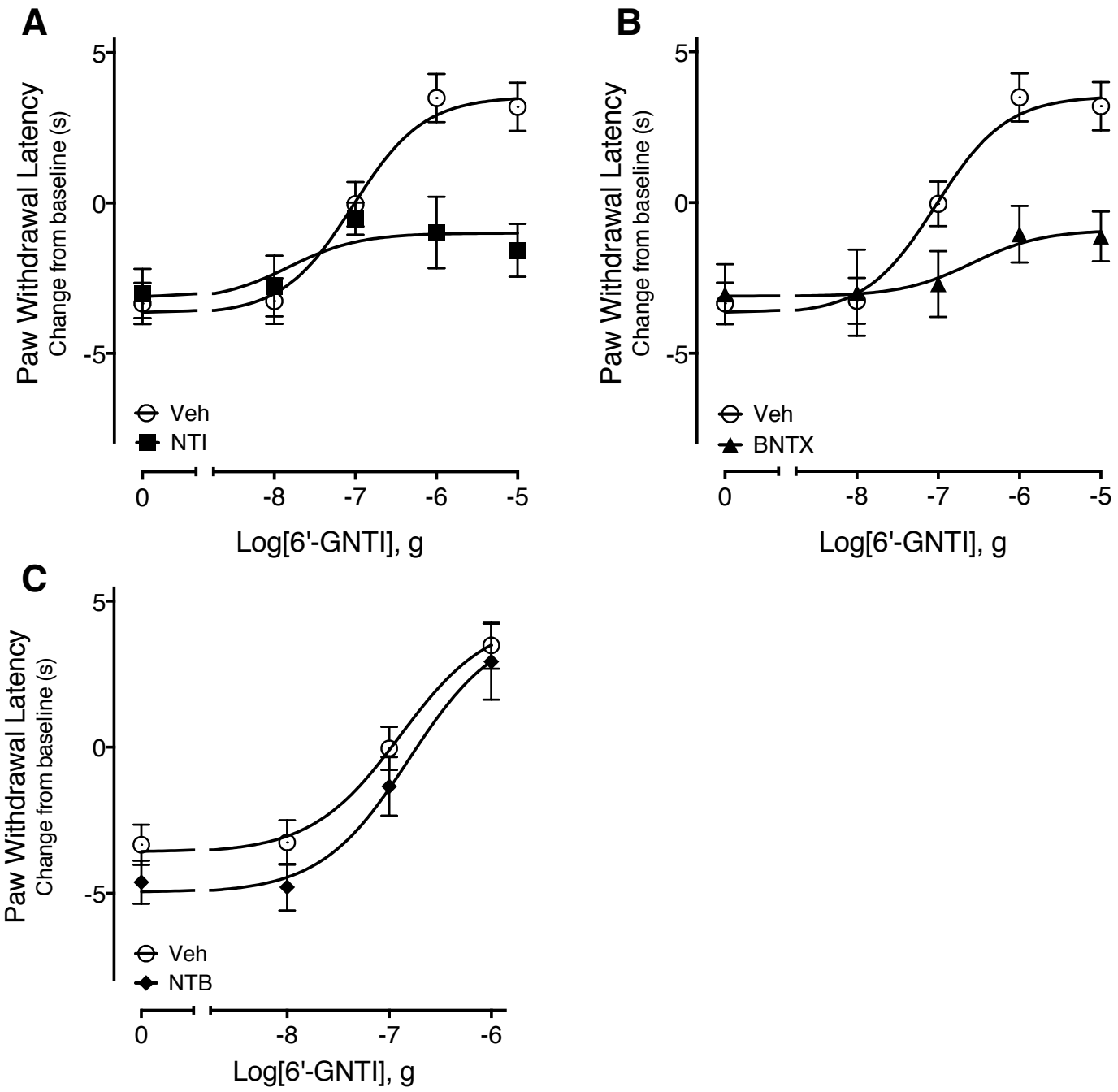

Figure 7

Molecular Pharmacology Fast Forward. Published on February 7, 2018 as DOI: 10.1124/mol.117.109975
This article has not been copyedited and formatted. The final version may differ from this version.

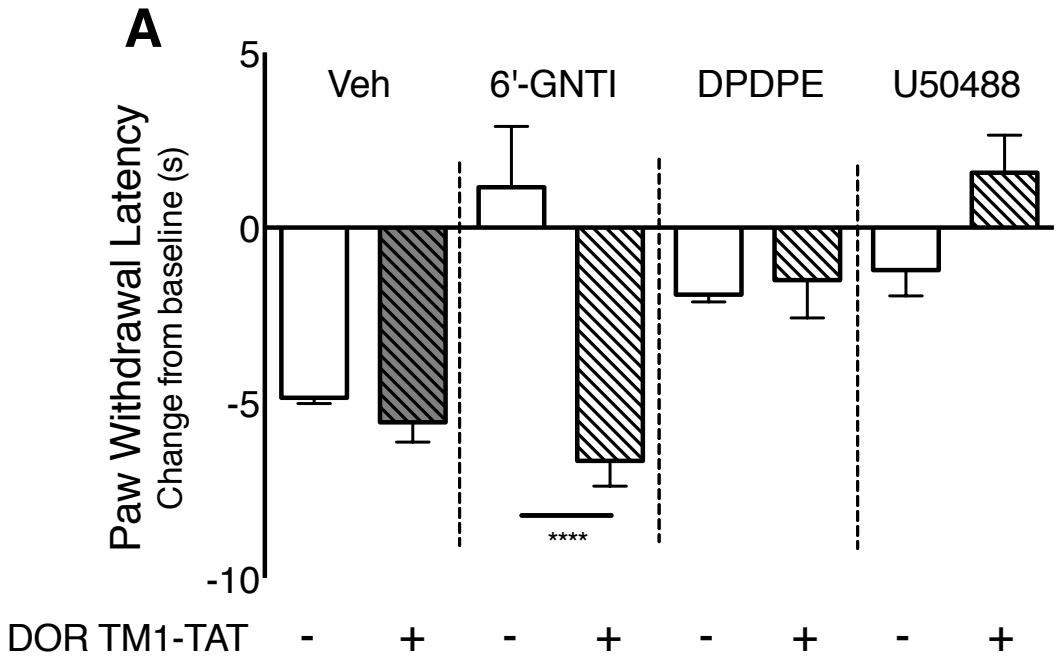

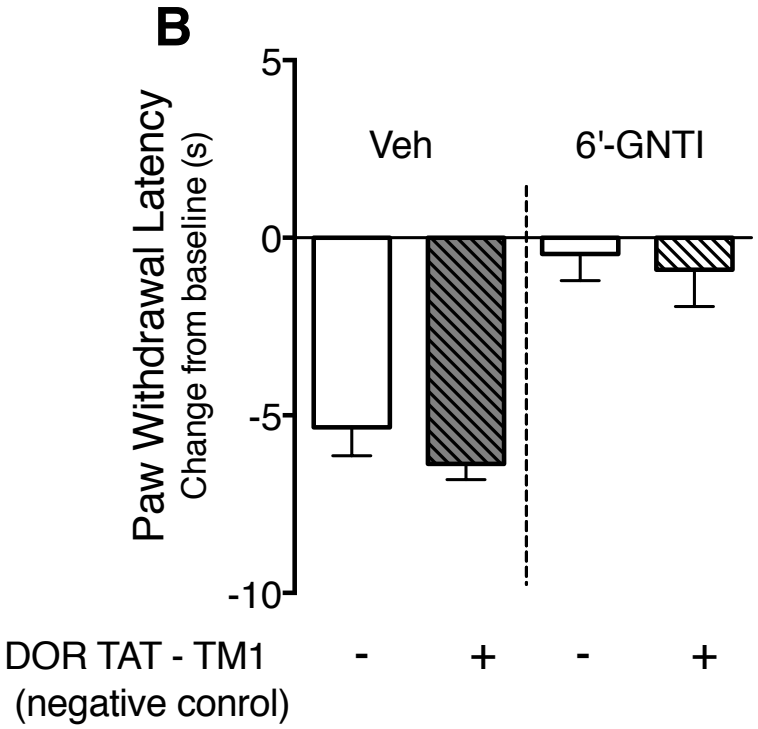

Figure 8

Molecular Pharmacology Fast Forward. Published on February 7, 2018 as DOI: 10.1124/mol.117.109975
This article has not been copyedited and formatted. The final version may differ from this version.

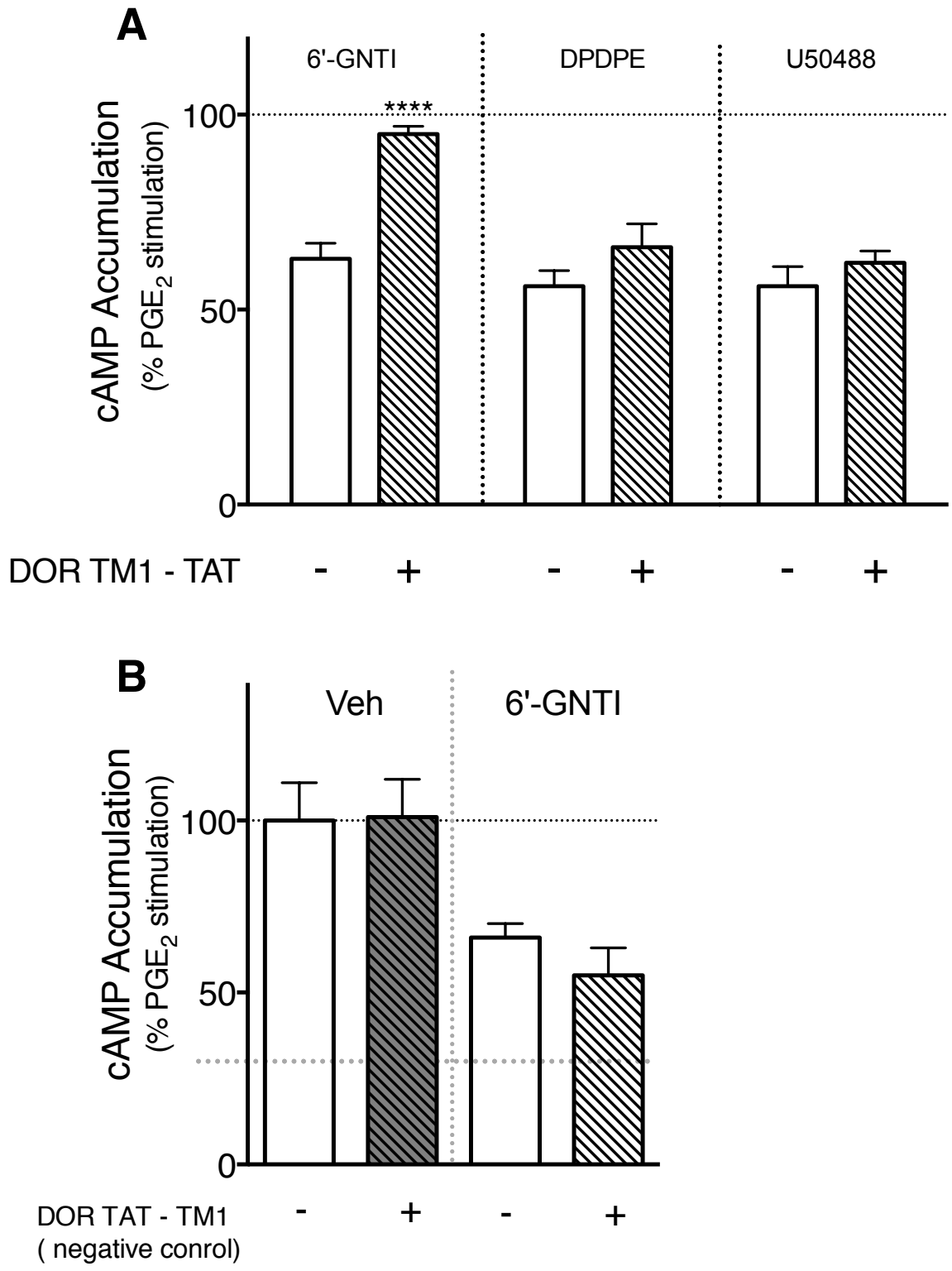

Figure 9

Title: Allosterism within delta opioid-kappa opioid receptor heteromers in peripheral sensory neurons: Regulation of kappa opioid agonist efficacy

Authors: Blaine A. Jacobs, Miryam M. Pando, Elaine Jennings, Teresa A. Chavera, William P. Clarke and Kelly A. Berg

Journal Name: Molecular Pharmacology

Supplemental Figure Legends

Supplemental Figure 1. The DOR antagonists, BNTX, NTI, and NTB, block DPDPE-mediated inhibition of PGE_2-stimulated cAMP accumulation. Primary cultures of peripheral sensory neurons were pretreated with vehicle (Veh), BNTX (200 nM, 100 x Ki), NTI (20 nM, 100 x Ki), or NTB (1 nM, 100 x Ki) for 15 min. After pretreatment, cells were incubated with PGE_2 (1 μM) with or without a maximal dose of DPDPE (100 nM) and cellular cAMP levels measured 15 min later. Data are expressed as the percentage of PGE_2-stimulated cAMP levels and are the mean ± SD, n=2. *P<0.05; **P<0.01 vs. Veh pretreatment group. One-way ANOVA with Dunnett's post test.

Supplemental Figure 2. The effect of the DOR antagonist naltrindole (NTI) on a subthreshold concentration of the KOR agonist, ICI-199441 (ICI) is saturable. Primary cultures of peripheral sensory neurons were pretreated with vehicle (Veh) or with either 0.2 nM, 2 nM, 20 nM or 100 nM Naltrindole (NTI) for 15 min. After pretreatment, cells were incubated with PGE_2 (1 μM) with or without a subthreshold concentration (1 nM) of ICI-199441 or a maximal concentration of ICI-199441 (1 μM) and cellular cAMP levels were measured 15 min later. Data are expressed as the percentage of PGE_2-stimulated cAMP levels and are the mean ± SEM, n=3. *P < 0.05; **P<0.01; ****P < 0.0001 vs 1 nM ICI alone; $^{+}$P < 0.05; $^{++}$P < 0.01; $^{+++}$P < 0.001; $^{++++}$P < 0.0001 vs. 1 μM ICI (one-way ANOVA with Dunnett's post test). The EC_{50} for NTI to enhance 1 nM ICI 199441 was 0.4 nM as determined with non-linear regression analysis.

Supplemental Figure 3. The DOR antagonists, BNTX, NTI, and NTB, block DPDPE–mediated antinociception. (A). The DOR antagonist alone did not alter baseline PWL (B). **A)** Rats received an intraplantar injection of vehicle (Veh), NTB (1 µg), NTI (40 µg), or BNTX (1 µg) 15 min before intraplantar co-injection with PGE_2 (0.3 µg) and a maximal dose of DPDPE (20 µg or vehicle (Veh). PWL was measured before and at 5 min intervals after the injection of PGE_2±DPDPE/Veh for 20 min. Data are expressed as the change (seconds) from individual pre-injection baseline values 10-min post DPDPE/Veh administration and represent mean ± SEM of 6 animals per group. One-way ANOVA with Dunnett's post test *$P<0.05$ PGE_2-DPDPE vs. PGE_2 - Veh. **B)** Rats received an intraplantar injection of vehicle (Veh), NTB (1 µg), NTI (40 µg), or BNTX (1 µg). PWL was measured before and at 5 min intervals after the injection, for 20 min.

Supplemental Figure 4. Timecourse curves for the effect of the DOR antagonist, NTI, on inhibition of PGE_2-evoked thermal allodynia by the KOR agonist, ICI-199441. To induce opioid receptor functional competence, rats received an intraplantar pre-injection with BK (25 µg) along with vehicle **(A)** or NTI (40 µg) **(B)** 15 min before intraplantar co-injection with PGE_2 (0.3 µg) and the indicated doses (µg) of ICI 199441. PWL was measured before injections (baseline) and at 5 min intervals following injections for 20 min after the last injection. BK produced a transient allodynia (decrease in PWL) that returned to baseline before injection of PGE_2±ICI 199441. Data are expressed as the change (seconds) from individual pre-injection baseline values for each dose at each timepoint and represent mean ± SEM of 6-9 animals per group.

Supplemental Figure 5. Timecourse curves for the effect of the DOR antagonist, NTI, on inhibition of PGE_2-evoked thermal allodynia by the KOR agonist, U50488. As described in

Supplemental Figure 4, rats received an intraplantar pre-injection with BK (25 µg) along with vehicle **(A)** or NTI (40 µg) **(B)** 15 min before intraplantar co-injection with PGE_2 (0.3 µg) and the indicated doses (µg) of U50488. PWL was measured before injections (baseline) and at 5 min intervals following injections for 20 min after the last injection. Data are expressed as the change (seconds) from individual pre-injection baseline values for each dose at each timepoint and represent mean ± SEM of 6-9 animals per group

Supplemental Figure 6. Timecourse curves for the effect of the DOR antagonist, BNTX, on inhibition of PGE_2-evoked thermal allodynia by the KOR agonist, U50488. Rats received intraplantar injection with BK (25 µg) along with vehicle **(A)**, BNTX (1 µg) **(B)** or BNTX (1 µg) + NTI (40 µg) **(C)** 15 min before intraplantar co-injection of PGE_2 (0.3 µg) and the indicated doses of U50488. PWL was measured before injections (baseline) and at 5 min intervals following injections for 20 min after the last injection. Data are expressed as the change (seconds) from individual baseline values for each dose at each timepoint and represent mean ± SEM of 6-9 animals per group.

Supplemental Figure 7. Efficacy of the DOR-KOR heteromer bivalent agonist, KDAN-18, requires both DOR and KOR in peripheral sensory neurons. Primary cultures of peripheral sensory neurons were transfected with siRNA directed against DOR (gray), KOR (white), or non-targeting siRNA as a control (black). Five days after transfection, inhibition of PGE_2-stimulated cAMP accumulation in response to KDAN-18 (10 and 100 nM) was measured. Data are expressed as the percentage of PGE_2-stimulated cAMP levels and are the mean ± SD, n=2 independent experiments. $^*P < 0.01$ vs. off-target (control) siRNA, one-way ANOVA with Dunnett's post test.

Supplemental Figure 8. Timecourse curves for the effect of the DOR antagonists, NTB, NTI, and BNTX, on inhibition of PGE_2-evoked thermal allodynia by 6'-GNTI. As described in Supplemental Figure 4, rats received intraplantar injection of BK (25 µg) along with vehicle **(A)**, NTB (1 µg) **(B),** NTI (40 µg) **(C)**, or BNTX (1 µg) **(D)** 15 min before intraplantar co-injection of PGE_2 (0.3 µg) and the indicated doses of 6'-GNTI. PWL was measured before injections (baseline) and at 5 min intervals following injections for 20 min after the last injection. Data are expressed as the change (seconds) from individual baseline values for each dose at each timepoint and represent mean ± SEM of 6-12 animals per group.

Supplemental Figure 9. Timecourse curves for the effect of the DOR TM1-TAT peptide on inhibition of PGE_2-evoked thermal allodynia by DPDPE, U50488, and 6'-GNTI. A-D) Rats received an injection of BK (25 µg, i.pl.) in combination with either vehicle, or the DOR TM1-TAT-peptide (3.94 µg) followed 30 min later with a co-injection of PGE_2 (0.3 µg) with vehicle **(A)**, DPDPE (20 µg) **(B)**, U50488 (0.1 µg) **(C),** or 6'-GNTI (1 µg) **(D)**. **E)** Rats received an injection of BK (25 µg, i.pl.) in combination with either vehicle, or the negative control DOR TAT-TM1 peptide (3.94 µg) followed 30 min later with a co-injection of PGE_2 (0.3 µg) with vehicle or 6'-GNTI (1 µg). PWL was measured before injections (baseline) and at 5 min intervals following injections for 20 min after the last injection. Data are expressed as the change (seconds) from individual baseline values for each dose at each timepoint and represent mean ± SEM of 6 animals per group.

Title: Allosterism within delta opioid-kappa opioid receptor heteromers in peripheral sensory neurons: Regulation of kappa opioid agonist efficacy

Authors: Blaine A. Jacobs, Miryam M. Pando, Elaine Jennings, Teresa A. Chavera, William P. Clarke and Kelly A. Berg

Journal Name: Molecular Pharmacology

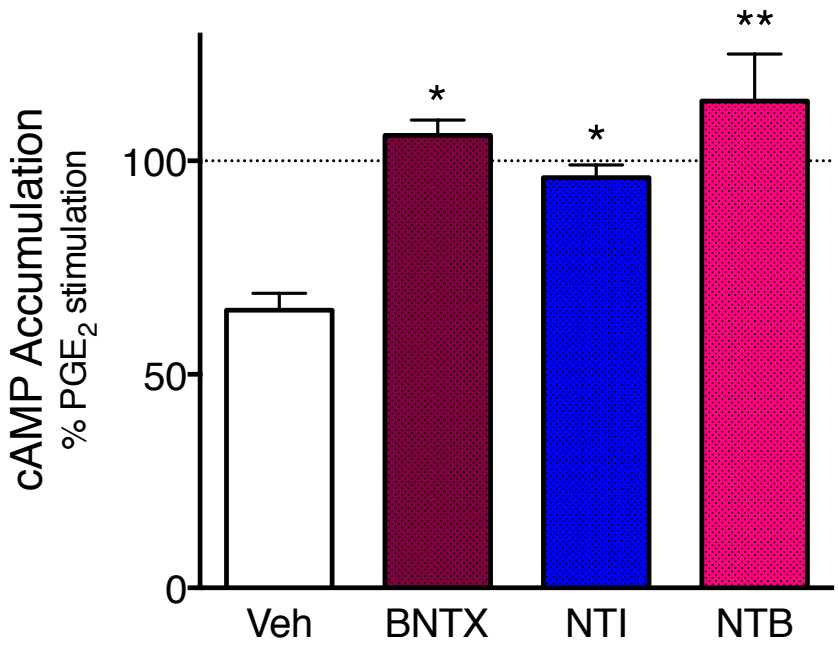

Supplemental Figure 1

Title: Allosterism within delta opioid-kappa opioid receptor heteromers in peripheral sensory neurons: Regulation of kappa opioid agonist efficacy

Authors: Blaine A. Jacobs, Miryam M. Pando, Elaine Jennings, Teresa A. Chavera, William P. Clarke and Kelly A. Berg

Journal Name: Molecular Pharmacology

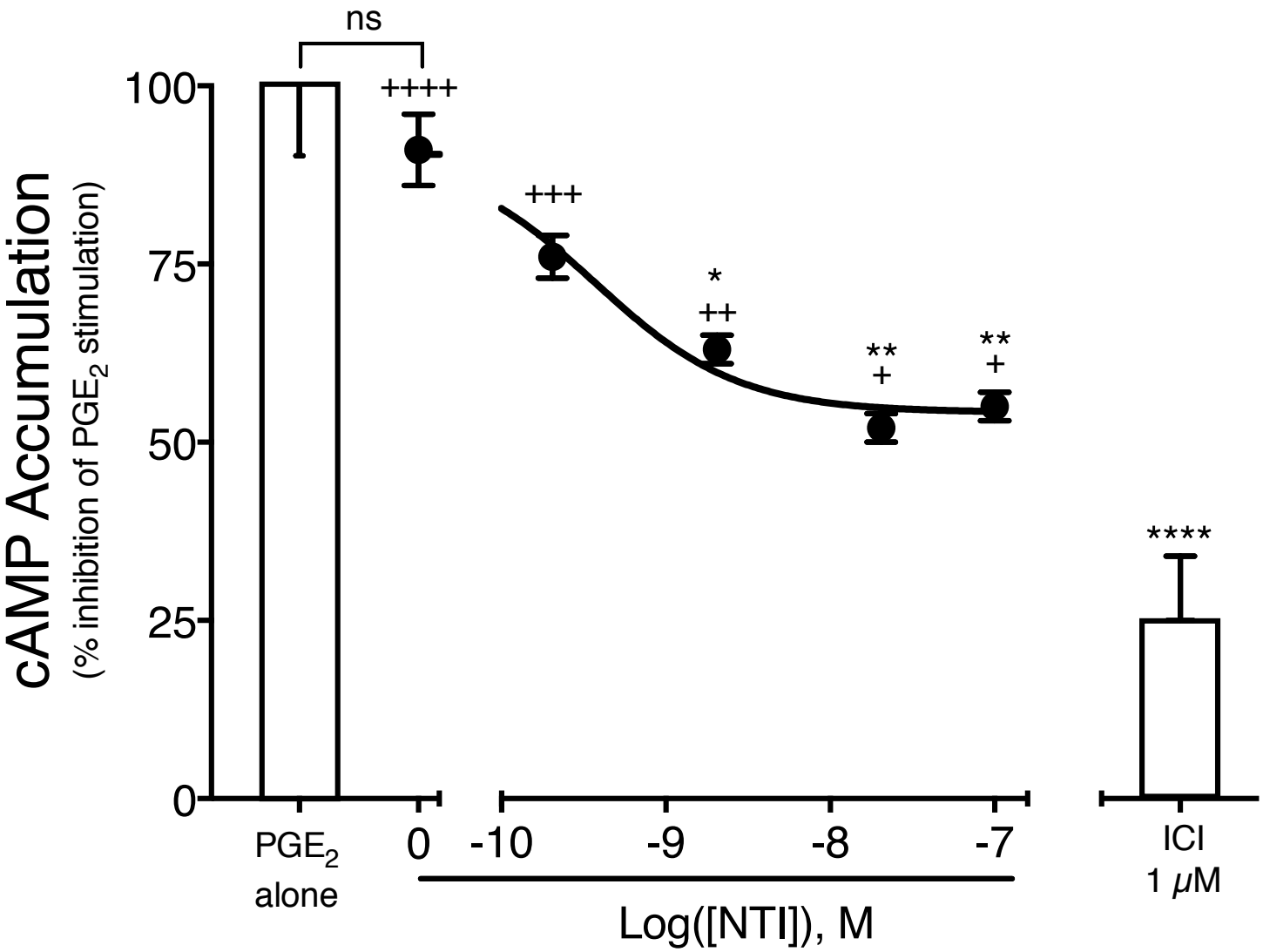

Supplemental Figure 2

Title: Allosterism within delta opioid-kappa opioid receptor heteromers in peripheral sensory neurons: Regulation of kappa opioid agonist efficacy

Authors: Blaine A. Jacobs, Miryam M. Pando, Elaine Jennings, Teresa A. Chavera, William P. Clarke and Kelly A. Berg

Journal Name: Molecular Pharmacology

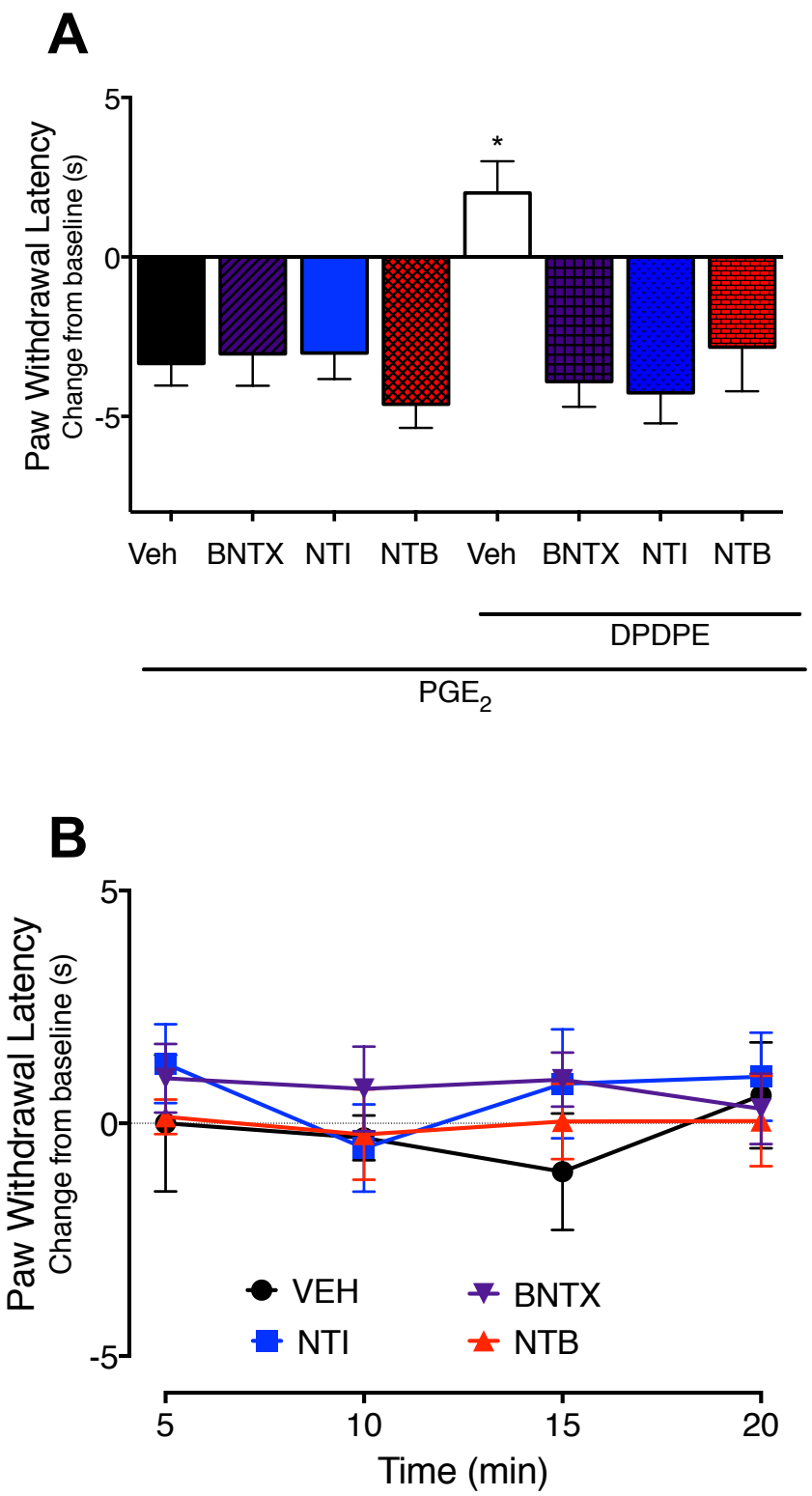

Supplemental Figure 3

Title: Allosterism within delta opioid-kappa opioid receptor heteromers in peripheral sensory neurons: Regulation of kappa opioid agonist efficacy

Authors: Blaine A. Jacobs, Miryam M. Pando, Elaine Jennings, Teresa A. Chavera, William P. Clarke and Kelly A. Berg

Journal Name: Molecular Pharmacology

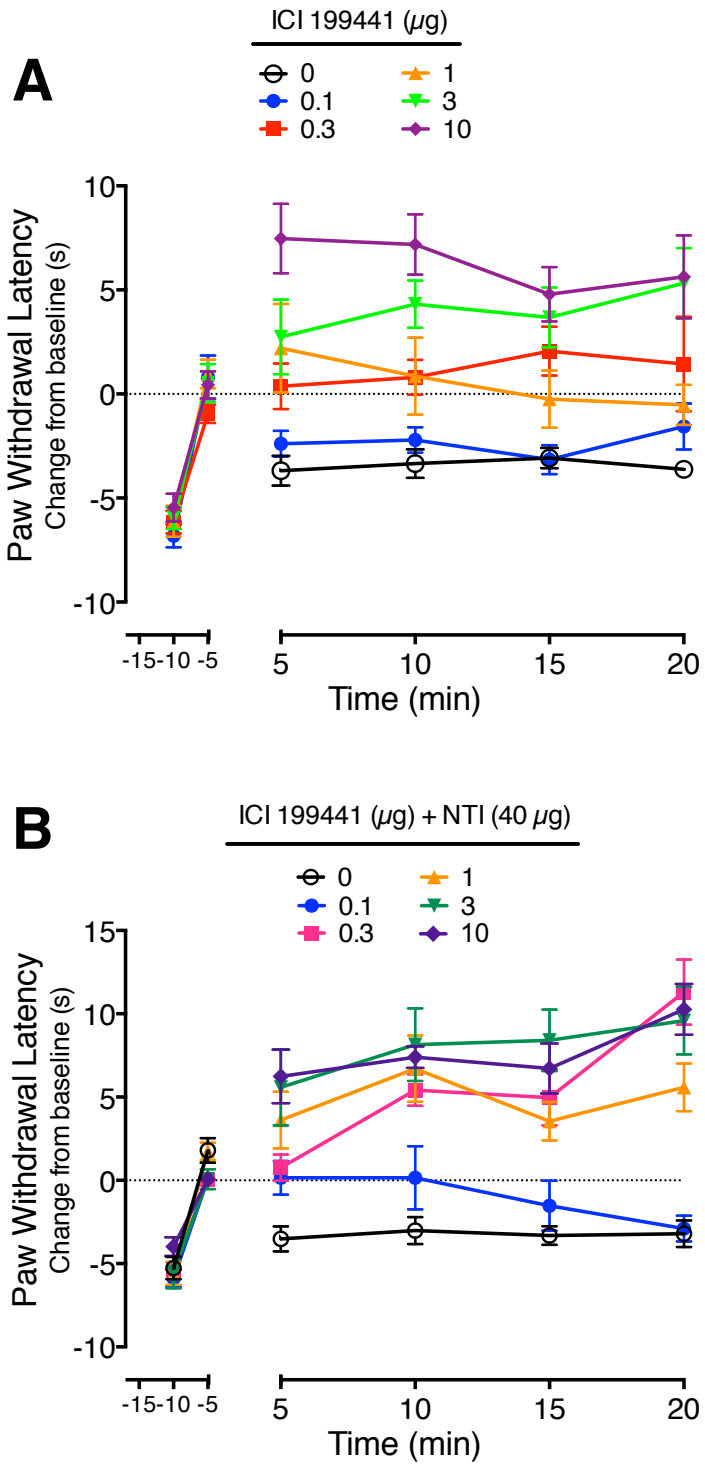

Supplemental Figure 4

Title: Allosterism within delta opioid-kappa opioid receptor heteromers in peripheral sensory neurons: Regulation of kappa opioid agonist efficacy

Authors: Blaine A. Jacobs, Miryam M. Pando, Elaine Jennings, Teresa A. Chavera, William P. Clarke and Kelly A. Berg

Journal Name: Molecular Pharmacology

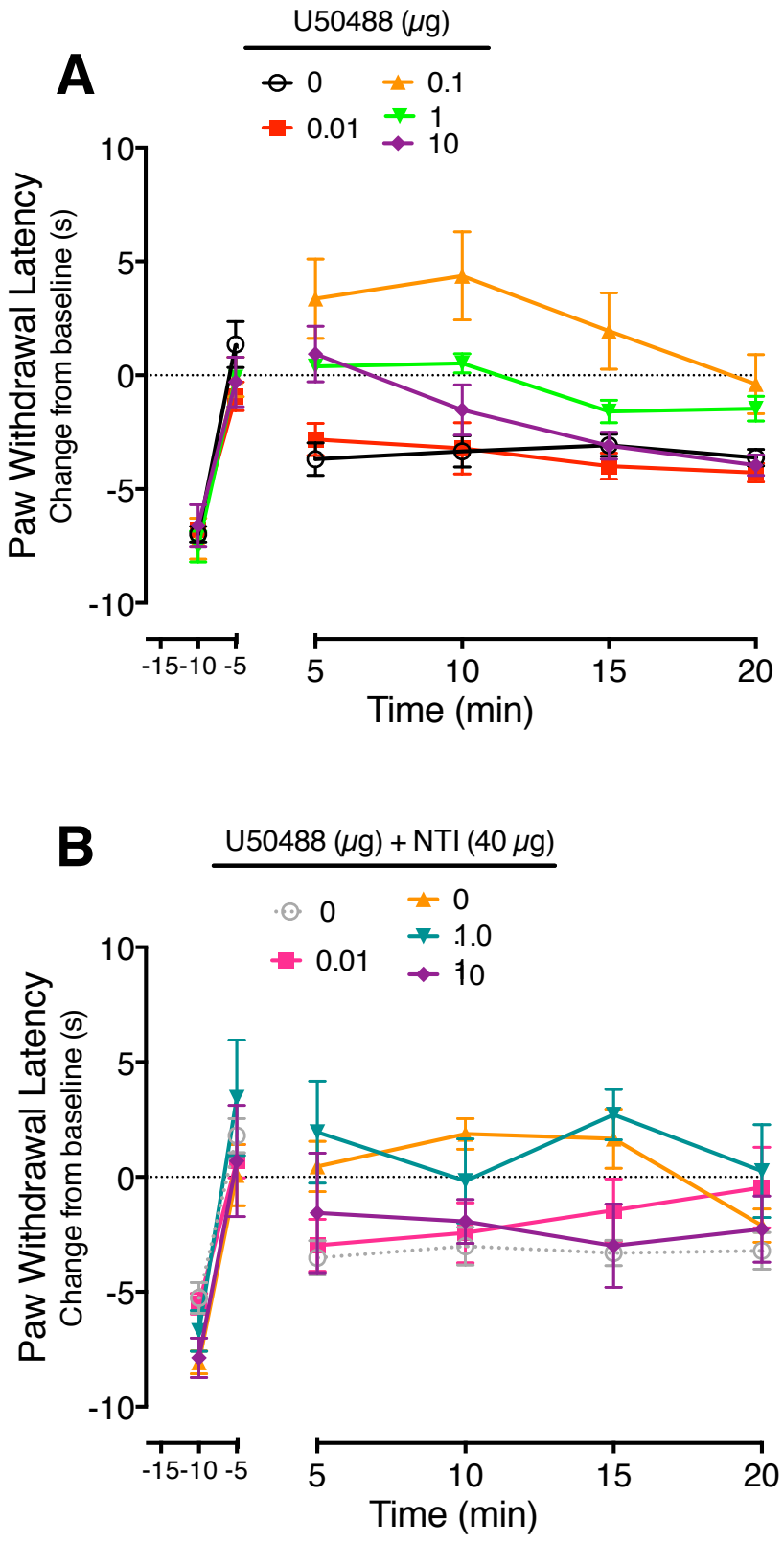

Supplemental Figure 5

Title: Allosterism within delta opioid-kappa opioid receptor heteromers in peripheral sensory neurons: Regulation of kappa opioid agonist efficacy

Authors: Blaine A. Jacobs, Miryam M. Pando, Elaine Jennings, Teresa A. Chavera, William P. Clarke and Kelly A. Berg

Journal Name: Molecular Pharmacology

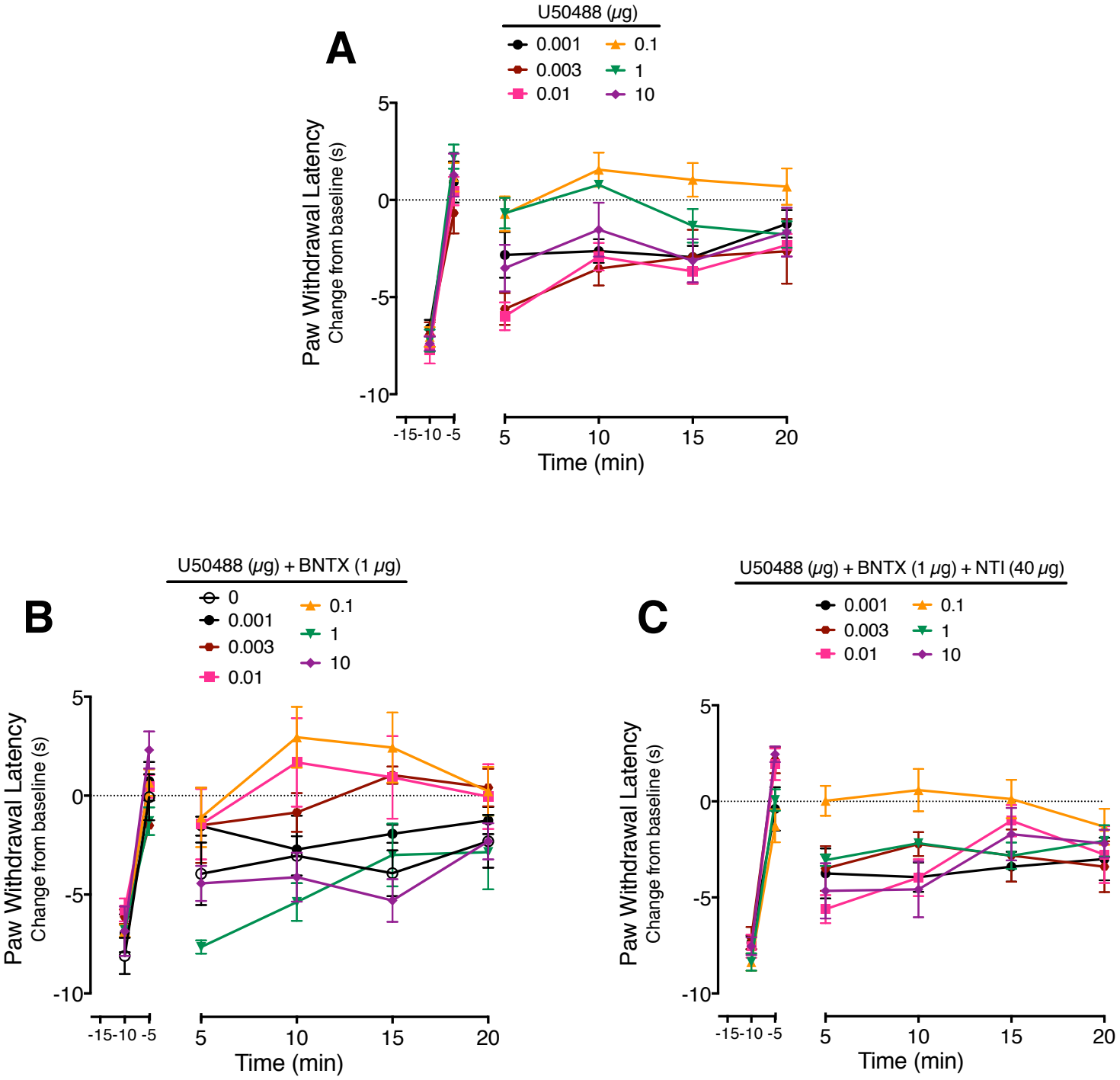

Supplemental Figure 6

Title: Allosterism within delta opioid-kappa opioid receptor heteromers in peripheral sensory neurons: Regulation of kappa opioid agonist efficacy

Authors: Blaine A. Jacobs, Miryam M. Pando, Elaine Jennings, Teresa A. Chavera, William P. Clarke and Kelly A. Berg

Journal Name: Molecular Pharmacology

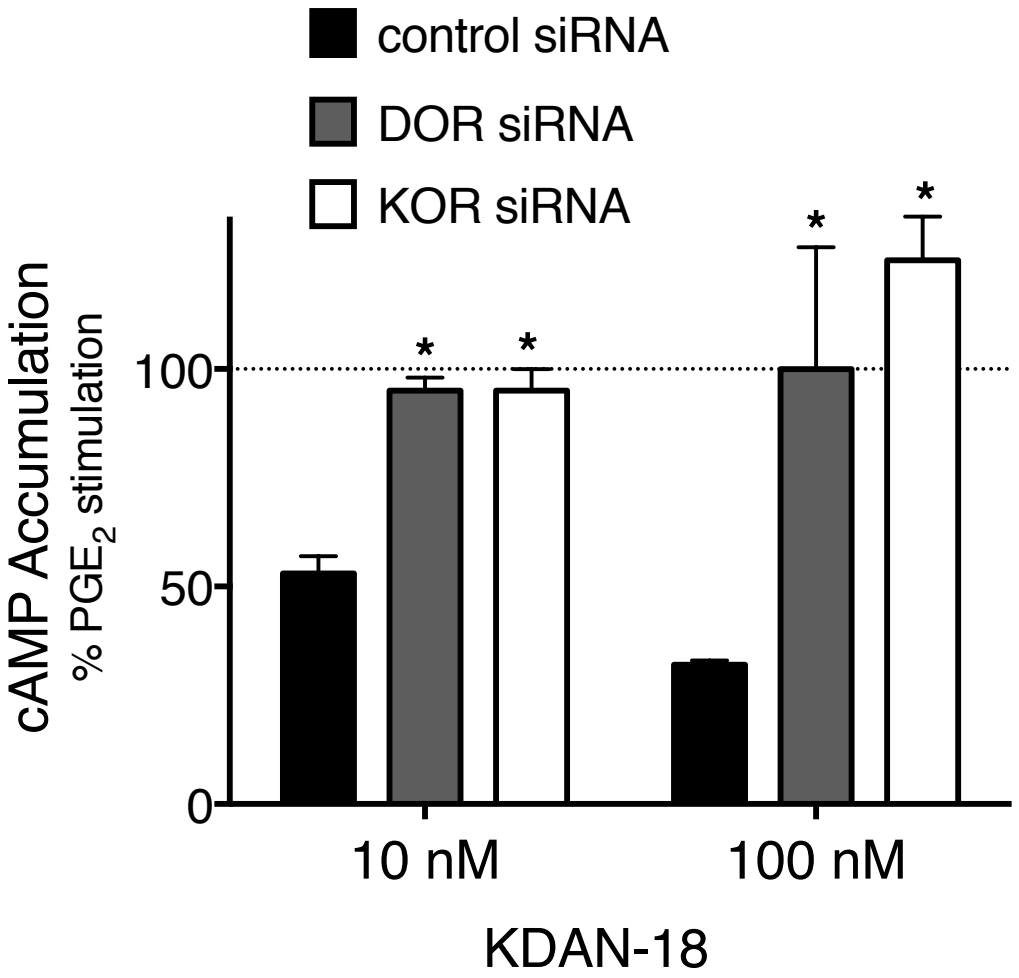

Supplemental Figure 7

Title: Allosterism within delta opioid-kappa opioid receptor heteromers in peripheral sensory neurons: Regulation of kappa opioid agonist efficacy

Authors: Blaine A. Jacobs, Miryam M. Pando, Elaine Jennings, Teresa A. Chavera, William P. Clarke and Kelly A. Berg

Journal Name: Molecular Pharmacology

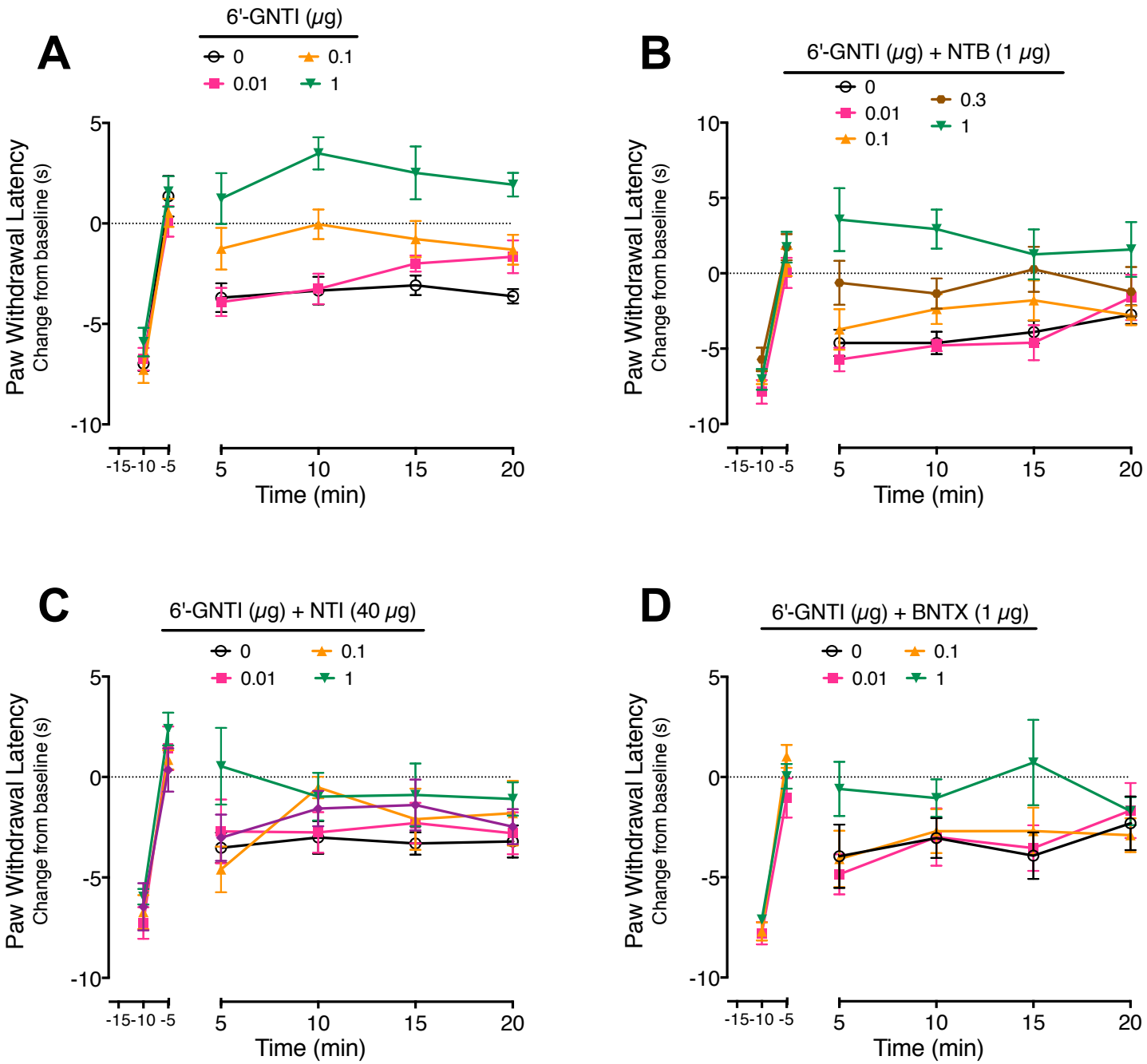

Supplemental Figure 8

Title: Allosterism within delta opioid-kappa opioid receptor heteromers in peripheral sensory neurons: Regulation of kappa opioid agonist efficacy

Authors: Blaine A. Jacobs, Miryam M. Pando, Elaine Jennings, Teresa A. Chavera, William P. Clarke and Kelly A. Berg

Journal Name: Molecular Pharmacology

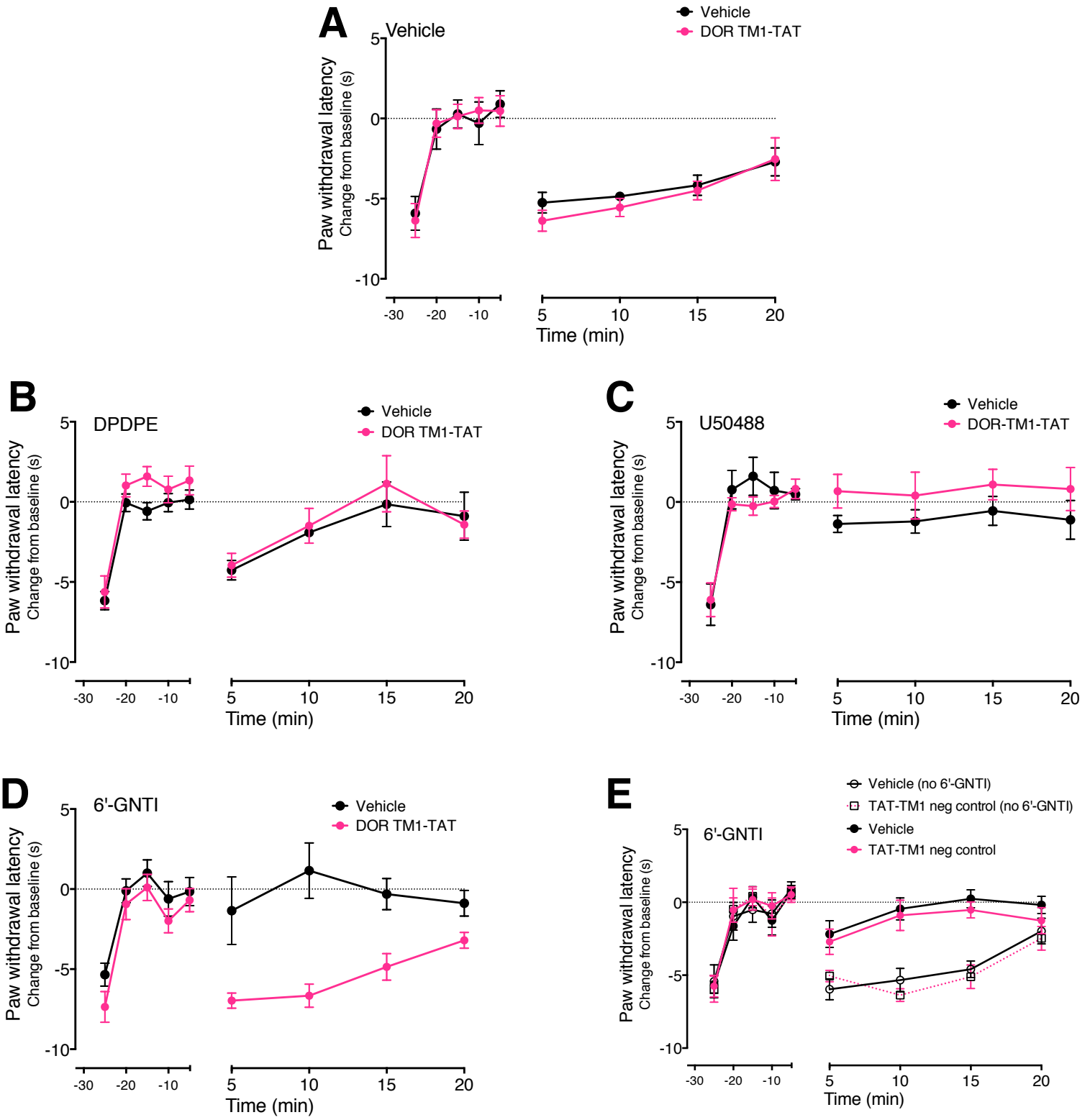

Supplemental Figure 9